Sol-gel Method Synthesis and Characterization of ZnO Nanoparticles for the use in Optoelectronic Devices

Dechasa Tolera Fufa

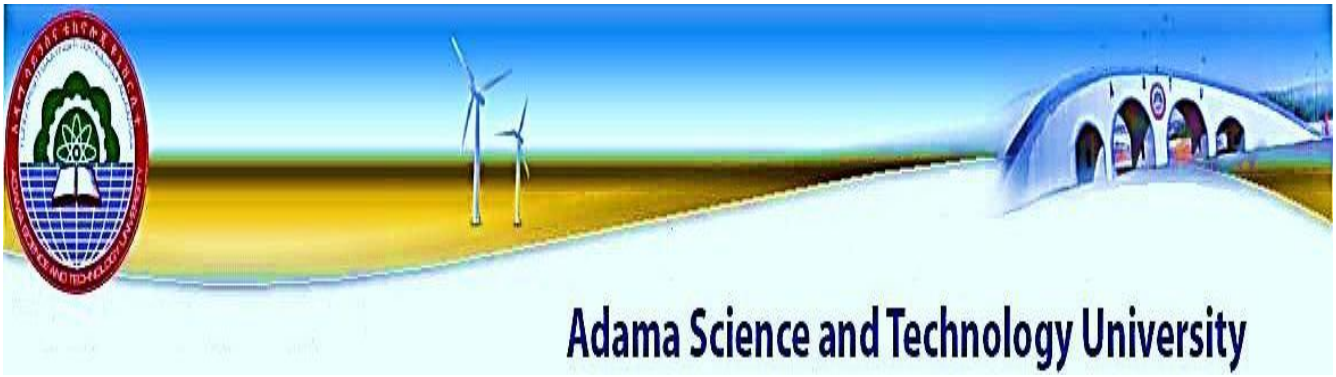

Adama, Ethiopia

Sol-gel Method Synthesis and Characterization of ZnO Nanoparticles for the use in Optoelectronic Devices

Submitted in partial fulfillment of the requirements for the degree of

Master of Science in Physics (Material Science)

By

Dechasa Tolera Fufa

Advisor: Dr. Megersa Wodajo Shura

August 2016

SCHOOL OF GRADUATE STUDIES

ADAMA SCIENCE AND TECHNOLOGY UNIVERSITY

As thesis research advisor, I hereby certify that I have read and evaluated this thesis entitled: "**Sol-gel Method Synthesis and Characterization of ZnO Nanoparticles for the use in Optoelectronic Devices**" prepared under my guidance by Dechasa Tolera. I recommend that it can be submitted as fulfilling the thesis requirement.

Dr. Megersa Wodajo _____ _____

Advisor Signature Date

As members of the Board of Examiners of the M.Sc. thesis Open Defense Examination, we certify that we have read and evaluated the thesis work prepared by Dechasa Tolera and examined the candidate. We recommended that the thesis be accepted as fulfilling the thesis requirement for the Degree of Master of Science in Physics.

_____ _____ _____

Chairperson Signature Date

_____ _____ _____

Internal Examiner Signature Date

_____ _____ _____

External Examiner Signature Date

DECLARATION AND STATEMENT OF THE CANDIDATE

First, I declare that this thesis is my authentic work and all sources of materials used for the thesis work have been duly acknowledged. This thesis has been submitted in partial fulfillment of the requirements for M.Sc. degree at the Adama Science and Technology University (ASTU) and is deposited at the University Library to be made available to borrowers under rules of the Library. I solemnly declare that this thesis work is not submitted to any other institution anywhere for the award of any academic degree, diploma, or certificate.

Brief quotations from this thesis are allowable without special permission provided that accurate acknowledgement of source is made. Requests for permission for extended quotation from or reproduction of this manuscript in whole or in part may be granted by the head of major department or the Dean of the School of Graduate Studies when in his or her judgment the proposed use of the material is in the interests of scholarship. In all other instances, however, permission must be obtained from the author.

Name of candidate: Dechasa Tolera Fufa Signature: _____

Place: Adama Science and Technology University, Adama

Date of Submission: August, 2016

ACKNOWLEDGEMENTS

First and foremost, I would like to be grateful for loving, kindness, of the Almighty God in bestowing me health, strength, patience and protection throughout my study period.

Next, I would like to start with my advisor Dr. Megersa Wodajo for his professional and endless support and patience, faithful and immense affection to help me from the beginning to the end of my study in the program of material science. Once again, I would like to express my sincere gratitude to him for his valuable guidance, inspiration and great material support throughout my entire thesis work. This work has been in its present shape with considerable professional and material inputs from various sources. Therefore, it is amazing excitement to me to come this final point and to express my deepest gratitude to all individuals and organizations who contributed directly or indirectly to this study and the production of this thesis work. I would also like to express my gratitude to Dr.S.Sambasivam for his all technical supports to sample synthesis at chemistry post graduate and research laboratory, Adama.

I would like to acknowledge the Adama Science and Technology University for extending all its supports to accomplish this work. Last but not least, my heartfelt gratitude goes to fellow friends and colleagues. They deserve special thanks for their valuable contributions and encouragement.

Table of Contents

List of Figures

List of Tables

List of Acronyms

XRD -X-Ray Diffraction

TEM -Transmission Electron Microscope

SEM Scanning Electron Microscope

UV-VIS -Ultraviolet Visible

PL – Photoluminescence

1D - One dimensional

CBM - Conduction band minimum

HCP - Hexagonal close packed

NBE - Near band edge emission

VBM - Valance band maximum

FWH M- Full Width Half Maximum

ZnO- Zinc Oxide

KeV- Kilo Electron Volt

nm -Nanometer

E_g - Band gap Energy

LED- Light Emitting Diodes

NBE-Near band emission

Abstract

The precursors used in the preparation were zinc hexahydrate, sodium hydroxide, and methanol (as it is without purification). Citric acid was added during preparation for the sake of molecule disperser purpose and surface modification. ZnO nanoparticles have been successfully synthesized by the sol gel method. The main motivation for this thesis is not only to successfully realize the controllable synthesis of ZnO nanoparticles, but also to investigate the structure, optical and electrical properties in detail by means of scanning electron microscopy (SEM),transmission electron microscopy (TEM), photoluminescence (PL) spectroscopy and X-ray diffraction (XRD) and UV-Vis absorbance in the ZnO nanoparticle is demonstrated. The effect of annealing temperatures on the morphology, optical and electrical properties of the nanoparticles were also systematically studied. Different techniques are used to investigate the performance of ZnO nanoparticles use in optoelectronic devices such as light emitting diodes, laser diodes, and photoconductivity.

X- ray diffraction (XRD) indicated that all the grown ZnO nanoparticles produced was crystallize in the wurtzite structure and post growth annealing does not significantly enhance the crystalline quality of the material. The effect of annealing temperatures on the morphology of grown ZnO nano particles was examined by using scanning electron microscope (SEM) and transmission electron microscope (TEM).

The optical quality of ZnO nanoparticle was carefully examined using photoluminescence (PL). The PL analysis showed that the nanoparticles have the same characteristics as that of bulk ZnO, except for the stronger contribution from surface related bound excitons in the former case. Surface adsorbed impurities causing depletion and band bending in the near surface region is implied from both UV and PL. Regardless of the annealing environment, annealing at a temperature as low as 300°C enhances the UV emission and suppresses defect related deep level emission. However, annealing above 500°C is required to out-diffuse hydrogen presence, which is in the low temperature PL spectra of ZnO.

Key words: Sol-gel method, Characterization techniques, ZnO Nano particles, Optoelectronic devices, Electrical and Optical properties and annealing temperature.

Chapter 1

Introduction

1.1 Background

Nowadays, the world is surmounting on the roof of technology and electronics, mostly dominated by compatible electronic equipment and thereby creating the need for materials possessing versatile properties. After digging the pages of history for the search of such type of material, a very common category of material comes out that is “semiconductor”. Thereby, the products of semiconductor industry spread all over the world and deeply penetrating into the daily life of human being. Since then, the semiconductor industry has kept growing enormously. The starting point of semiconductor industry was the invention of the first semiconductor transistor at Bell Lab in 1947 []. In the 1970’s, the information age of human being was started on the basis of the stepwise appearance of quartz optical fiber, III-V compound semiconductors and gallium arsenide (GaAs) lasers.

During the development of the information age, silicon (Si) keeps the dominant place on the commercial market, which is used to fabricate the discrete devices and integrated circuits for computing, data storage and communication. Germanium get famous due to possession of property like low melting point and lack of natural occurring germanium oxide to prevent the surface from electrical leakage whereas silicon dominates the commercial market for its better fabrication technology and application to integrated circuits for different purposes. As time passes on, the rapid growing world demands speed along with technology. This need was very well fulfilled by GaAs which ease the path for the design of high speed and optoelectronic devices. GaAs which is a direct band gap semiconductor possessing higher carrier mobility and higher effective carrier velocity in comparison to Si makes it better suited for optoelectronic devices. But this do not lead to the completion of requirement for the future world, something more is required that is high temperature electronics devices. The world therefore now demands a material that should possess inherent properties like larger band gap, higher electron mobility as well as higher breakdown field strength. As the development of information technologies, the requirement of ultraviolet (UV)/blue light emitter applications became stronger and stronger which is beyond the limits of GaAs.

Therefore, the wide band gap semiconductors such as SiC, GaN and ZnO, that means the third generation semiconductors come forth and turn into the research focus in the field of semiconductor [1].

Wide band gap semiconductors have gained much attention during last decade because of their possible uses as optoelectronic devices in the short wavelength and ultraviolet (UV) portion of the electromagnetic spectrum. These semiconductors such as ZnSe, ZnS, GaN, and ZnO, have shown in Table 1-1with their similar properties, crystal structures and band gaps. So on making investigation about such a material the compound comes out called "Zinc Oxide" that is a wide gap semiconductor material very well satisfying the above required properties. Not only has this Zinc oxide possessed many versatile properties for UV electronics, spintronic devices and sensor applications. ZnO also has been commonly used in its polycrystalline form over hundred years in a wide range of applications. This ignites many research minds all over the world and creates enthusiasm to develop proper growth and processing techniques for the synthesis of Zinc oxide. Thus, the ZnO related research has once more increased rapidly.

Table 1-1: Comparison of different semiconductors

semiconductor	Crystal structure	Lattice parameter		Eg(atRT)	Melting temp.	Excitation binding energy	Dielectric constant	
		a	c				ε_0	ε_∞
ZnO	Wurtzite	3.250$\dot{A}$	5.206$\dot{A}$	3.37eV	2248K	60Mev	8.75	3.72
GaN	Wurtzite	31.89$\dot{A}$	51.85$\dot{A}$	3.4eV	1973K	21Mev	9.5	5.15
ZnSe	Zinc blendes	5.667$\dot{A}$	-	2.7eV	1790K	20Mev	7.1	5.3
ZnS	Zinc blendes	3.824 $\dot{A}$	6.261$\dot{A}$	3.7eV	2103K	36Mev	9.6	5.7

The number of articles published on ZnO has increased every year and in 2007 ZnO became the second most popular semiconductor materials after Si. On one hand, the popularity to a large extent is due to the improvements in growth of high quality, single crystalline ZnO in both epitaxial layers and bulk form. On the other hand, especially since the emergence of the nanotechnology, novel electrical, mechanical, chemical and optical properties are introduced

with the reduction in size, which are largely believed to be the result of surface and quantum confinement effects [1].Since, the development of nano-crystalline materials is a recent thrust area of research. ZnO is an important semiconductor, which has a direct band gap (3.37eV at room temperature), large bond strength, large excitation binding energy (E_b = 60meV) and high melting temperature (2248 K) [3]. ZnO has been widely used in many applications such as transparent conductive films, varistors, solar cell windows, bulk acoustic wave devices, lasers and diodes [1, 4].

In materials science, ZnO is often called a II-VI semiconductor because of zinc and oxygen belong to the II and VI groups of the periodic table respectively [2].Zinc oxide is an inorganic compound usually appears as a white powder, nearly insoluble in water. The powder is widely used as an additive into numerous materials and products including plastics, ceramics, glass, cement, rubber (e.g. car tyres), lubricants, paints, ointments, adhesives, sealants, pigments, foods (source of Zn nutrient), batteries, ferrites, fire retardants, etc. ZnO is present in the Earth crust as a mineral zincite; however, most ZnO used commercially is produced synthetically. The characteristics of ZnO powder depend on its size and methods of preparation. ZnO nanomaterial, in comparison to the bulk form of ZnO, have shown novel properties for some special applications in the fields of nano-electronics, ultraviolet lasing, frequency conversion, nanoscale optical circuitry and so on [5-9].

ZnO nanoparticles can be prepared on a large scale at low cost by simple solution-based synthesis methods, such as chemical precipitation [10, 11, 17], sol gel synthesis [13, 14] and hydrothermal reaction [15, 16, 17, 18]. However, agglomeration and secondary growth often occur in these ZnO nanoparticles when we dry the wet particles separated from the reaction solution. This is because large numbers of hydroxyl groups exist on the wet particle surface. Therefore, in simple wet chemical synthesis, grinding processing has been routinely used as a scalable physical technique to directly break bulk materials to form fine particles, but it is unsuitable for preparing nanoparticles [19].

In the present study, a simple and cost effective sol-gel method was used to prepare ZnO nanoparticles using zinc nitrate hexahydrate, and sodium hydroxide as a precursor, citric acid as

the complexing agent and a surfactant and methanol as a solvent. Therefore, that was the reason why sol-gel synthesis method was preferred as a method of ZnO nanoparticles synthesis.

1.2 Objectives of the Research work

The general objective of this research work is to investigate the optical properties, particle size, and crystallinity of the sol-gel method grown ZnO nanoparticles by using X-Ray Diffraction (XRD), SEM and TEM, PL and UV-Vis characterization techniques.

The specific objectives of this research work are to:

- Preparation of the ZnO nanoparticles by sol-gel method. Zinc nitrate hexahydrate and sodium hydroxide are the precursor's materials here.
- Determining the crystal structure and particle size with X-Ray Diffraction (XRD).
- Characterize the surface morphology of the ZnO nanoparticles by SEM and TEM.
- Determine the band gap from the spectral data by UV-Vis spectroscopy.
- Study the effect of post growth treatment on the structural, optical and electrical quality using XRD, SEM, TEM, PL and UV-Vis characterization techniques.

Chapter 2

Literature Review

2.1 Nanotechnology and Nano Science

Over the last two decades, science and technology has shown tremendous improvement in the hope of presenting the true secrets of the nature in molecular or atomic level [2, 3]. The principles of physics, as far as I can see, do not speak against the possibility of miniaturizations of things atom by atom." these are the words which buried the seed for nano-technology in the scientific mind of number of researchers who were attending the talk of famous physicist Richard Feynman when he mentioned "to synthesize nanoscale building blocks with precisely controlled size and composition, and assemble them into larger structures with unique properties and functions" in 1959 [22, 64]. In 1959, Richard Feynman gave a lecture titled "there's plenty of room at the bottom", suggesting the possibility of manipulating things at atomic level. This is generally considered to be the foreseeing of nanotechnology. However, the real burst of nanotechnology did not come until the early 1990s. Thus, after sophisticated instruments such as scanning electron microscopy and transmission electron microscopy, a characterization and manipulation became more available for researchers to approach the nanoworld [10, 65].

Nanotechnology makes us to believe that we would have the ability to create anything that we could precisely define. Nanotechnology [4, 66] is defined as the study of manipulating matter on the atomic and molecular scale. Nano science is the study of the behavior of objects at a very small scale, roughly 1 to 100nm. Nano science represents a revolution in constructing devices with atomic precision [20]. But Nanotechnology is the science of the small; the very small. It is the use and manipulation of matter at a tiny scale. At this size, atoms and molecules work differently and provide a variety of surprising and interesting uses. The progress of technology and quality of life of mankind has always been closely knit with the progress in material science and material processing technology. Most material processing techniques are based on breaking up large chunk of a material into desired shapes and sizes, inducing strain, lattice defects and other deformations in the processed material. Recent developments in nanotechnology and the demonstration of various quantum size effects in nanoscale particles, implies that most of the novel devices of the future will be based on properties of nanomaterial [21, 64, 65, 66].

2.2 Properties of Nanoparticles

The term nanoparticles are sometimes referred to as Nano powder, Nano crystals or Nano clusters. Nanoparticles are particles that have one dimension that is 100nm or less in size. The properties of many conventional materials change when formed from nanoparticles. This is typically because nanoparticles have a greater surface area per weight than larger particles; this causes them to be more reactive to certain other molecules [64]. Nanoparticles are used, or being evaluated for use, in many fields. Nanoparticles are of great scientific interest as they are effectively a bridge between bulk materials and atomic or molecular structures [65, 66].

A bulk material should have constant physical properties regardless of its size, but at the nano-scale size-dependent properties are often observed. Thus, the properties of materials generally change as their size approaches the nanoscale and as the percentage of atoms at the surface of a material starts to become significant. For bulk materials larger than one micrometer (or 1micron), the percentage of atoms at the surface is insignificant in comparison to the number of atoms in the bulk of the material [7, 64]. The interesting and sometimes unexpected properties of nanoparticles are therefore largely due to the large surface area of the material, which dominates the contributions made by the small bulk of the material. The high surface area to volume ratio of nanoparticles provides a tremendous driving force for diffusion, especially at elevated temperatures. Nanoparticles of usually yellow gold and gray silicon are red in color; gold nanoparticles melt at much lower temperatures (nearly 300℃ for 2.5nm size) than the gold slabs (1064℃); and absorption of solar radiation in photovoltaic cells is much higher in materials composed of nanoparticles than it is in thin films of continuous sheets of material, the smaller the particles, the greater the solar absorption [69]. Nanoparticles also often possess unexpected optical properties as they are small enough to confine their electrons and produce quantum effects. Moreover, nanoparticles have been found to impart some extra properties to various day to day products. For example, the presence of titanium dioxide nanoparticles imparts what we call the self-cleaning effect, and the size being nano range, the particles cannot be observed. Zinc oxide particles have been found to have superior UV blocking properties compared to its bulk substitute [63].

2.3 Band Structure in Nano materials

Nanometer range semiconducting materials have been a subject of intense study for last several years due to their size dependent physical and chemical properties [37– 40] below a critical size characteristic of the material. Blue shift in the optical absorption spectrum, size dependent luminescence, enhanced oscillator strength; nonlinear optical effects are some examples of the interesting properties exhibited by these Nano crystallites. All these properties are various manifestations of the so called size quantization effect which arises due to the increasing quantum confinement of the electrons and holes with diminishing size of the crystallites and the consequent changes in the electronic structures. Their electronic structure is between that of a molecule and bulk, giving rise to profound modifications of the physical properties.

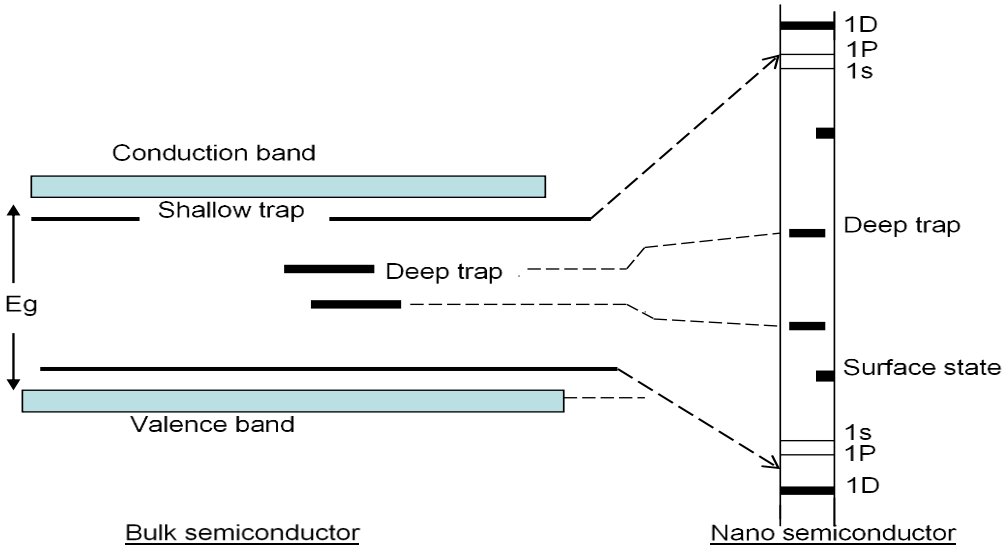

Figure 2-1: Energy level diagram comparing of bulk and small cluster of semiconductors [37-40].

Due to the finite size of the Nano crystals, the continuous energy bands of the bulk crystal transforms into a series of discrete states resulting in widening of the effective band gap. This is normally observed through optical absorption studies in which the lowest allowed absorption shifts to the higher energies [21] as the particle size decreases. Energy level diagram of the bulk and small clusters of semiconductors is shown in Figure2-1. The increase in the energy separation between valence states and excited energy levels is consequence of quantum confinement.

In any material substantial variation of fundamental, electrical and optical properties with size is observed when the diameter of the Nano crystals is comparable to or smaller than the diameter of the bulk excitons such that the energy levels spacing exceeds the thermal energy $k_B T$[22].

For a given temperature, this occurs at a very large size in semiconductors as compared to metals or molecular crystals, the nearest neighbour interactions are weak and the bands in the solid are very narrow and as a consequence not much size variations in optical and electrical properties are expected or observed in the Nano crystals regime. However, in case of metals, the edge of the band develops first and the center develops last upon decreasing size. Further, the Fermi level lies in the center of the band and the relevant energy level spacing is still very small and at temperatures above a few Kelvin, the electrical and optical properties more closely resemble those of a continuum, even in relatively small sizes. In semiconductors, however, the Fermi level lies in between two bands, so that the edges of the bands dominate the optical and electrical behavior.

2.4 Overview of ZnO Materials

ZnO is an inorganic compound also known as zincite and occurs rarely in nature, generally in a crystalline form. It is usually orange or red in color due to presence of manganese impurity. It usually appears as a white crystalline powder, which is nearly insoluble in water. Most of ZnO which is used commercially is produced synthetically. ZnO is actually a wide band gap semiconductor of the II-VI semiconductor group. Thereby, it has several favorable properties like high electron mobility, good transparency, wide band gap for semi-conductivity, high room-temperature luminescence, etc. Because of its unique properties and versatile applications, it is used in transparent electronics, ultraviolet (UV) light emitters, piezoelectric devices and chemical sensors. These remarkable physical properties form the basis for motivation of device miniaturization has been made large effort on the synthesis, characterization and device applications of ZnO nanomaterial.

2.5 Physical Properties of ZnO

Important physical parameters of ZnO are summarized in Table 2-1 It should be noted that there is still uncertainty in some of these values, e.g. hole mobility, thermal conductivity, etc. ZnO possesses the following physical properties [2]:

- Molecular Weight: $\frac{81.37g}{mol}$
- Color: Pure microcrystalline zinc oxide is white. Single crystal zinc oxide is colorless. Zinc oxide turns lemon yellow on heating and reverts to white on cooling.
- Relative Density: $5.607 g/cm^3$
- Vapor Pressure (1500^{o}C): 12mm.
- Zinc oxide sublimes at atmospheric pressure and at temperatures over 1200℃. Heat of Sublimation was between 1350℃ and 1500℃ at 129 Kcal/mole (vapor not disassociated) and 193 Kcal/mole (vapor associated).
- Heat Capacity: $C_p = \frac{9.62 \text{cal}}{\text{deg}}$ at 25℃
- Coefficient of Thermal Expansion $\alpha = 4 \times 10^{-6}$/℃

Table 2-1: Some basic properties of ZnO.

	Physical Parameter	Value
1	Lattice parameters in (nm) at 300K	$a = 0.32495, c = 0.52069, \frac{a}{c} = 0.625, u = 0.380$
2	Density g/cm^3	5.606
3	Stable phase	Wurtzite
4	Melting point (˚C)	1975
5	Thermal conductivity W/K.cm	0.6-1.2
6	Linear expansion coefficient (/°C)	a: 6.5×10^{-6}, c: 3.0×10^{-6}
7	Static dielectric constant	8.656
8	Refractive index	2.008-2.029
9	Energy band gap (eV)	3.3714, direct
10	Excitons binding energy (meV)	60
11	Electron effective mass (m_o)	0.24
12	Electron Hall mobility cm^2/Vs	200
13	Hole effective mass (m_o)	0.59
14	Hole Hall Mobility cm^2/Vs	5-50

(m_o is the free electron mass)

2.6 Crystal structure and lattice parameters of ZnO

The first enthusiasm started studies of the lattice parameter by M.L. Fuller in 1929 and C. W. Bunn‟s study in 1935, but the enthusiasm flagged with the difficulty in producing high quality crystal crystalline material. Zinc oxide has the wurtzite hexagonal crystal structure. Zinc oxide usually crystallizes in three different forms: hexagonal wurtzite, cubic zinc blende and cubic rock salt. The latter is the most rarely found. The wurtzite structure is most stable at ambient conditions and is hence most common. In an ideal wurtzite crystal with a hexagonal close-packed lattice type has lattice parameters, a_0= 0.32495nm and c_0 = 0.52069nm, in the ratio of a_0/c_0=0.625, and it belongs to the space group of II-VI [33, 35] and is characterized by two interconnecting sub lattices of Zn^{2+} and O^{2-} where each anion is surrounded by four cations at the corners of a tetrahedron with a typical sp^3covalent bonding. The structure of ZnO can be described as a number of alternating planes composed of tetrahedral coordinated O^{2-} and Zn^{2+} ions, stacked alternately along the C-axis (Figure 2-).

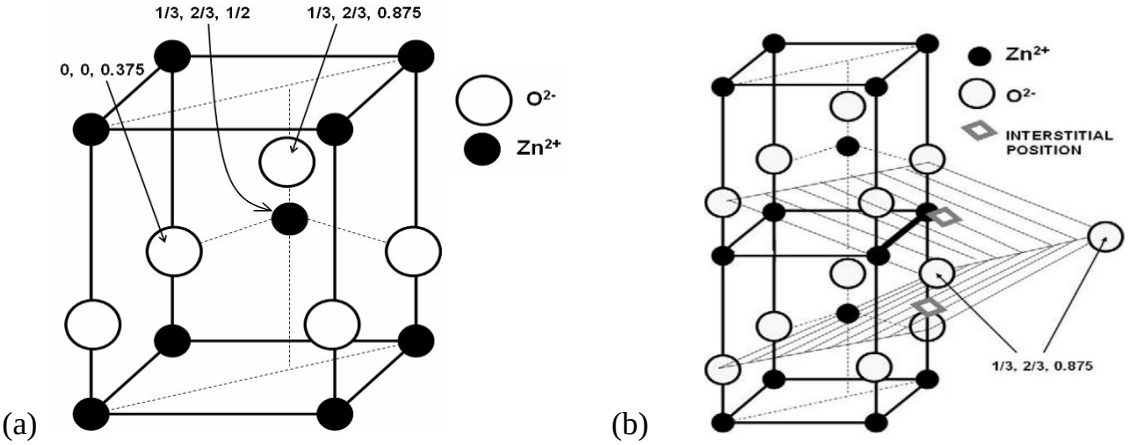

Figure 2-2: (a) ZnO unit cell with ionic positions of zinc and oxygen atoms, (b)Zinc interstitial sites in the ZnO wurtzite lattice. Redrawn from [47]

The room-temperature lattice parameters determined by various experimental measurements and theoretical calculations for the wurtzite ZnO are in good agreement with each other. The lattice constants mostly range from 3.2475 to 3.2501Å for the a-parameter and from 5.2042 to 5.2075Å for the c-parameter.

The measure of the amount by which each atom is displaced with respect to next along the c-axis is given by the parameter u, and experimentally, zinc oxide wurtzite structure is found to have $u = \frac{a}{c} = \frac{3}{8} = 0.38$ in fractional coordinates. The internal parameter u is defined as the length of the bond parallel to the c-axis (anion–cation bond length or the nearest-neighbor distance) divided by the c-lattice parameters. The basal plane lattice parameter (the edge length of the basal plane hexagon) is universally depicted by a; the axial lattice parameter (unit cell height), perpendicular to the basal plane, is universally described by c. Each sub-lattice includes four atoms per unit cell, and every atom of one kind (group II atom) is surrounded by four atoms of the other kind (group VI), or vice versa, which are coordinated at the edges of a tetrahedron.

2.7 Mechanical Properties

Its elastic constants are relatively smaller than those of other III-V semiconductors, e.g. GaN. The high heat capacity and high heat conductivity, low values of thermal expansion and high melting points are some of the characteristics of ZnO. This makes it an important material for many piezoelectric applications, which require a high degree of electromechanical coupling among them.

2.8 Piezoelectric effect and Polar Surfaces

Piezoelectricity of ZnO has been extensively studied for various applications in force sensing, acoustic wave resonator, acousto-optic modulator, etc. The origin of the piezoelectricity lies due to its crystal structure, in which the oxygen atoms and zinc atoms are tetrahedrally bonded. In such a structure which is non Centro symmetric, the center of positive charge and negative charge can be displaced due to external pressure induced lattice distortion. This displacement results in local dipole moments, thus a macroscopic dipole moment appears over the entire crystal. In fact, among the tetrahedrally bonded semiconductors, ZnO has the highest tensor which provides a large electro-mechanical coupling [3]. Another result of the non-Centro symmetric ZnO crystal structure is its spontaneous polarization and polar face dominated nanostructures. The crystal structure of ZnO can be visualized in a way that oxygen atoms and zinc atoms are tetrahedrally bonded. These tetrahedrons stack along a particular direction. Due to the effect of spontaneous polarization, the position of positive charge is displaced from that of negative charge in that fixed particular direction.

The net result of this spontaneous polarization is a charged ZnO surface. In order to achieve minimized energy, the charged surface results in unique nano-ring and nano-coil structure.

2.9 Optical Property of ZnO

The simplest experiment to determine the size dependence in semiconductor nanoparticles is to study absorption spectrum of a material as a function of wavelength of incident photons. The photons are absorbed only when their energy is equal or greater than the energy gap of the semiconductor $hv \geq E_g$. Therefore, there is a sudden rise in absorption when photon energy is same as energy gap. If the energy gap increases there is a shift in the onset of absorption towards shorter wavelength. As shown in figure 2-1 one expects a 'blue shift' in absorption in smaller and smaller clusters, which is indicative of increasing energy gap. The optical absorption spectra give the size quantization effect as well as the estimation of band gap.

The different energy states available between valence and conduction bands responsible for radiative recombination are provided by photoluminescence spectra. The Nano size quantized particles yield the best external photoluminescence quantum efficiency and luminescence decay time much faster than the corresponding bulk crystals. The luminescent measurements carried out on various nanocrystals show that the efficiency increases with decreasing size of the Nano crystalline particles. Highest occupied Molecular orbital (HOMO) and lowest unoccupied Molecular orbital (LUMO) instead of top of valence band and bottom of conduction band in case of extended solid respectively. The band gap of semiconductors and the optical transparency behavior of materials could be changed by controlling the grain size in the nano crystalline state for small particle sizes. On the other hand, when the grain size is much smaller than the wavelength of light, scattering does not take place and so the material is fairly transparent [24]. The optical absorption characteristics can also be modified by allowing interaction to occur between the Nano sized clusters [25]. The band gap becomes a function of the grain zone showing a 'Blue shift' with decrease in particle size. The size dependent optical absorption also shows changing colour of a material.

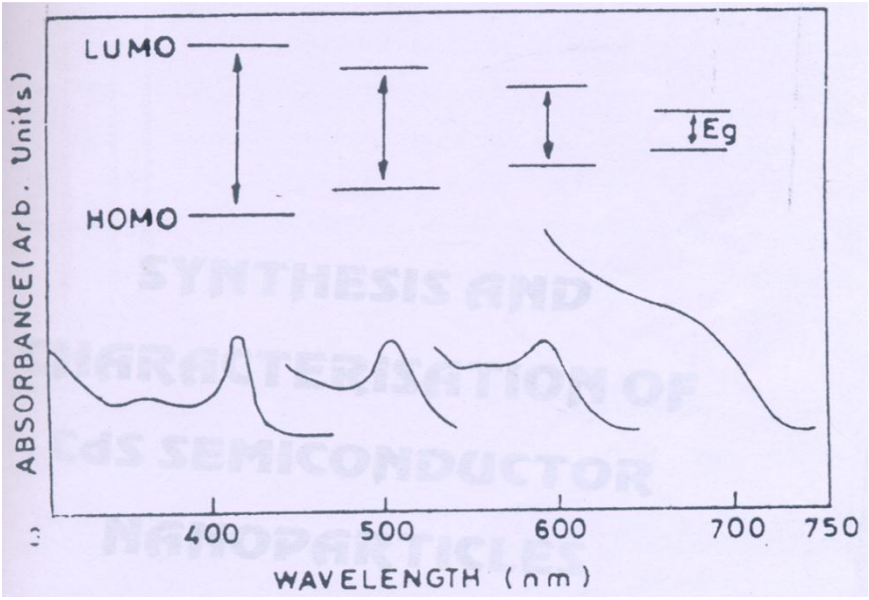

Figure 2-3: Optical absorption spectra for nanoparticles of different sizes [34, 42, and 46].

2.10 Electronic band structures in ZnO

Considering that ZnO is a candidate semiconductor for optoelectronic device applications, a clear understanding of the band structure is of critical importance in explaining the optical and electrical properties. Several theoretical approaches of varying degrees of complexity, involving the Local Density Approximation (LDA), the Self-interaction corrected Pseudo Potential (Sic-PP) method, or the empirical tight–binding Hamiltonian, have been employed to calculate the band structure [19]. Experimental data have also been published regarding the band structure and electronic states of wurtzite ZnO [20]. UV reflection/absorption or emission techniques have been used to measure the electronic core levels in solids. These methods measure the energy difference between the upper valence-band states and the bottom conduction-band states.

In ZnO, the valence band consists of three bands labeled A, B and C by spin-orbit and crystal-field splitting [42]. This splitting is schematically illustrated in Figure 2-4. The A and C sub-bands are known to possess Γ7 symmetry, while the B band has Γ9 symmetry. These three bands correspond to light hole (A), heavy holes (B) and the crystal field split band (C) [42]. The band splitting values are measured at 4.2 K [42].

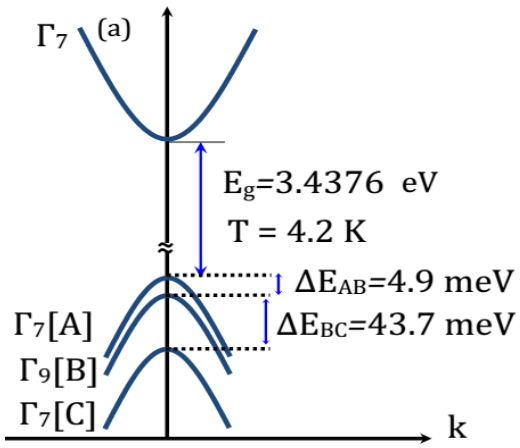

Figure 2-4: Low temperature band structure of ZnO showing valence band splitting into three (A, B, C) which is caused by crystal field and spin-orbit splitting [53].

The conduction band of wurtzite ZnO is constructed from s-like states and it is symmetrical about the Γ point while the valence band is constructed mainly from p-like states. The band structure E(k) for ZnO, calculated by using an empirical tight–binding Hamiltonian [42].The optical band gap between occupied and empty bands (i.e. in ZnO is about 3.37eV). This energy represents the energy difference between full and empty states. The top filled states are called the valence band and the maximum energy of the valence band of states is called the VBM. The lowest band of empty states above the gap is called the conduction band with the lowest point in that band called the CBM. In this figure, the VBM and CBM coincide at $\hbar k = 0$, at the Γ point indicating that ZnO is a direct band gap semiconductor. Where, k refers to the wave number, $\hbar$ refers to planks constant we can say the momentum is conserved. i.e. $\hbar k = 0$ implies that momentum is conserved.

2.11 Electrical Properties of ZnO

The fundamental study of the electrical properties of ZnO nanostructures is crucial for developing their future applications in Nano electronics. ZnO has a quite large band gap of 3.37eV at room temperature. The advantages of a large band gap include higher values of breakdown voltages, sustaining large electric fields, high-temperature and high-power operations. ZnO has n-type character, in the absence of doping. Non-stoichiometry is usually the origin of n-type character.

Due to defects such as oxygen vacancies and zinc interstitials, ZnO nanowires are reportedly show n-type semiconductor behavior. An n-type ZnO nanowire can serve as p-n junction diodes and light emitting diodes (LED) [4].

2.12 Chemical Properties of ZnO

ZnO has the following chemical properties [2]:

- ZnO occurs as the mineral zincite or as white powder known as zinc white. It is usually orange or red in color due to manganese impurity.
- Crystalline zinc oxide is thermo chromic, which changes from white to yellow colour when heated and reverting to white colour on cooling. This change in colour is caused by a very small loss of oxygen at high temperatures.
- Zinc oxide is amphoteric, that is it reacts with both acids and alkalis. With acid it reacts to form familiar compound such as zinc sulfate. With alkali it forms zincates.

$$ZnO + 2HCl \rightarrow ZnCl_2 + H_2O$$

$$ZnO + 2NaOH + H_2O \rightarrow Na_2(Zn(OH)_4)$$

- ZnO decomposes to form zinc vapor and oxygen at about 1975˚C indicating that its considerable stability. Heating with carbon converts ZnO into Zn, which is more volatile.

  $ZnO + C \rightarrow Zn + CO$
- The following reaction is extremely important in zinc pyro metallurgy

  $ZnO + CO \rightarrow Zn + CO_2$
- Commercial zinc oxide shows a measurable but low level of water solubility, 0.005 g/liter.
- Zinc oxide exposed to air absorbs both water vapor and carbon dioxide. This results [6] in the formation of basic zinc carbonate.

2.13 Quantum Confinement Effects

Quantum confinement occurs in nanocrystals when their size is reduced so that approaches the size of the excitons Bohr radius (the size of an excitons in a bulk crystal). ZnO, the excitons Bohr radius is ~ 2.34 nm [39]. PL can be used to observe the quantum confinement effect in nanostructures. However, there are few reports on this effect in ZnO nanostructures [39].

Experimental evidence of quantum confinement effects have been reported by Gue*t al.* [39], where PL and absorption spectra from Nano rods with radii of 1.1nm were found to be blue shifted compared to the spectra of bulk materials. Lu *et al.* [40] also observed quantum confinement effects in the PL spectra of quantum dots with diameter as large as 15nm and 6nm in height. The quantum dots studied by Lu *et al.*[39]exhibited a strong free excitons adsorption at 3.41eV at room temperature, significantly larger than that in bulk ZnO (3.37eV), representing a 90meV blue-shift.

2.14 Luminescence in ZnO

Light emission through any process other than blackbody radiation is called luminescence and requires external excitation as it is a non-equilibrium process. Based on the excitation source, luminescence is referred to either as photoluminescence (PL) (caused by absorption of photons), electroluminescence (EL) (caused by electric current), Cathodoluminescence (CL) (caused by an electron beam), chemo luminescence (caused by chemical reactions) or thermo luminescence (caused by heat). In this section, the basic principles of PL and the possible emission lines in ZnO are described. PL is a powerful tool to study point defects in wide-band gap semiconductors. Most of the experimental results on point defects in ZnO have been obtained from the analysis of mainly the PL data [44]. The principle of PL is straightforward.

Figure 2-shows the simplified band structure of a semiconductor near the Centre of the first Brillouin zone, where a material with band gap energy E_g is irradiatedby a laser with energy $h\nu \geq E_g$, resulting in the excitation of an electron into the conduction band (arrow 1) and leaving a hole behind in the valence band. An electron-hole (e-h) pair is thus generated. The electrons and holes thermalize to the lowest energy state of their respective bands via phonon emission shown by (the red-wave arrows)before recombining (arrow 2) across the fundamental band gap or the defect levels within the band gap and emitting photons of the corresponding energies in two basic mechanisms. These are radiative and non-radiative recombination. When the electron–hole recombination results in photon emission, the process is called radiative recombination. Recombination process that does not produce photons is known by non-radiative recombination in which the energy is exchanged with the lattice as heat through phonon emissions within defect states in semiconductor or transferred its energy to other carriers. On-radiative recombination occurs mainly through three physical mechanisms, but cannot be

detected by PL. These are Auger recombination, recombination at defects in the bulk, and surface recombination.

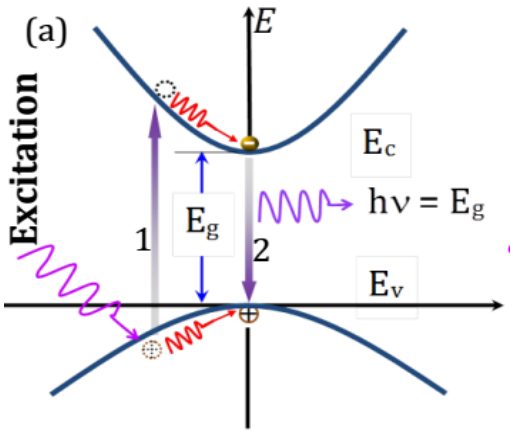

Figure 2-5: Band diagram illustration of the different processes that make up the photoluminescence spectra: excitation, relaxation and recombination in k-space [1, 3, 4].

During Auger recombination the e-h pair energy is transferred to a third free carrier that will move to a higher energy in the conduction band (in the case of an electron) or to a lower energy in the valence band (in the case of a hole). The e-h pair thus recombines without photon emission. This is a three-body process because an electron and two holes or a hole and two electrons are involved. Since this is a three-particle interaction, it is normally only significant in non-equilibrium conditions when the carrier density is very high. For this reason, it only occurs under very high injection levels or for materials with high equilibrium carrier concentrations.

Based on the wide band gap and non-degeneracy of the valence band (shown in section 2.2), it is suggested that Auger recombination is not important in ZnO. Recombination at defects in the bulk and surface regions of ZnO are expected to be the major non-radiative recombination processes. In particular, surface related non-radiative recombination is most pronounced in nanostructures.

2.15 Synthesis of ZnO Nanoparticles by Wet Techniques

These techniques are generally applicable for characterization by light scattering techniques. These are basically bottom-up approaches, that is, they begin with ions or molecules and gradually build them up into larger structures. These nanoparticles synthesizing techniques come under the colloid chemistry, and also involve classical sol-gel processes, or other aggregation

processes. These wet chemistry techniques synthesize the best quality nanoparticles. This is because of the following reasons [31]:

- This method produces nanoparticles which are in the form of a dispersion, hence high interparticle forces can be designed in order to prevent agglomeration.
- No formation of aggregates.
- The nanoparticles are mono disperse, that is, all are of the same size with small tolerances.
- The morphology and chemical composition can be minutely controlled. This is important for research purposes where the material quality must be very high to derive meaningful results.
- Some modifications were implemented to enhance the applications of ZnO nanoparticles, for instance controlling nanoparticles size by addition of surfactant and etc. Surfactant is a surface active agent that tends to reduce the surface tension of liquid and act as dispersant.

2.15.1The Chemistry Concerning of ZnO Nanoparticles

In the synthesis when $(Zn(NO_3)_2 \cdot 6H_2O)$ dissolves in water it dissociates into $Zn^{2+}$and$NO_3{}^{-}$. Since the main concern isZn^{2+}, which is a component of ZnO, let us proceed to what will happen to the zinc ions in the presence of water molecules. The neutral Zinc has the electronic structure:

$$Zn^0 \equiv 1s^2 2s^2 2p^6 3s^2 3p^6 4s^2 3d^{10}. \quad (2\text{-}1)$$

When Zn^{2+} ions form, Zn loses two of its valence electrons and the 4s-level orbitals are empty.

$$Zn^{2+} \equiv 1s^2 2s^2 2p^6 3s^2 3p^6 3d^{10}. \quad (2\text{-}2)$$

Zn then hybridizes (re-organizes the 4s, the 4p (4px, 4py, 4pz), and two of the 4d orbitals) to produce six new orbitals all with the same energy. It then uses six of these unpaired electronic states to accept lone pairs from six water molecules via co-ordinate bonding. In this configuration, the 2+ charge is no longer located entirely on the Zn, but is now spread over the whole of the ion. This makes the O–H bond in the water molecule even more polar and susceptible to further attacks. As a result, this compound loses its hydrogen to the nearby water molecules and acts as a hydrogen donor [41].The loss of hydrogen from such a complex continues until the stable $Zn(OH)_2$ compound is formed, as shown below:

$$[Zn(H_2O)_6]^{2+} \xrightarrow{H_2O} [Zn(H_2O)_5(OH)]^{+} \xrightarrow{H_2O} Zn(OH)_2(H_2O)_4$$

$$Zn(OH)_2(H_2O)_4 \equiv Zn(OH)_2 \leftarrow \text{PRECIPITATE}$$

In the absence of a strong base such as $OH^-$the deprotonation shown above is facilitated. However, in the presence of OH^- the zinc ion is more attracted to OH^-than H_2O. Thus, OH^- replaces the water ligand from the hexaqua-zinc complex ($[Zn(H_2O)_6]^{2+}$). The reaction is a simple ligand exchange. The ligand exchange reaction leading to the formation of ZnO can be summarized in the following reaction sequences [41].

$$[Zn(H_2O)_6]^{2+} \xrightarrow{(OH)^-} [Zn(H_2O)_5(OH)]^{+} \xrightarrow{(OH)^-} Zn(H_2O)_4(OH)_2$$

$$Zn(H_2O)_4(OH)_2 \equiv Zn(OH)_2 \xrightarrow{(OH)^-} [Zn(H_2O)_3(OH)_3]^{-} \xrightarrow{(OH)^-} [Zn(H_2O)_2(OH)_4]^{2-}$$

$$[Zn(H_2O)_2(OH)_4]^{2-} \xrightarrow{Temp} ZnO + H_2O$$

A sodium hydroxide is used as hydroxyl precursors in the present study, it is important to discuss the dissociation mechanisms of each precursor. Upon prolonged heat treatment, the dissociation steps of sodium hydroxide in water can be shown as:

$$NaOH \xrightarrow{H_2O} Na^{+} + OH^{-}$$

The possible pathway for the formation of ZnO using both precursors can be summarized as:

$$Zn(NO_3)_2 \rightarrow Zn^{2+} + 2{NO_3}^{-}$$

$$NaOH \rightarrow Na^{+} + OH^{-}$$

$$Zn^{2+} + 2OH^{-} \rightarrow Zn(OH)_2$$

$$Zn(OH)_2 \rightarrow Zn^{2+} + {(OH)_4}^{2-} \rightarrow ZnO + H_2O + 2OH^{-}$$

The chemical pathway leading to the formation of ZnO from sodium hydroxide and zinc nitrate hexahydrate involves the dissolution of sodium hydroxide upon prolonged heat treatment [37]) to form hydroxyl and hydrogen ions. The hydroxyl ions then react with Zn^{2+} ions to produce $Zn(OH)_4^{2-}$complexes, which are the precursors for the ZnO nanoparticles [41].

2.15.2 Synthesis of ZnO Nanoparticles by Sol-gel Method

Sol-gel method also known as chemical solution deposition is based on the hydrolysis of liquid precursors and formation of colloidal sols [26]. The formation of Nano size semiconductor or metal elements permits system with peculiar optical and electrical properties.

The possible reaction process and the formation of ZnO powders using both precursors can be summarized as; the zinc nitrate may convert into $Zn(OH)_2$ colloids firstly under alkali solution, as shown in reaction stage 1. During the process, part of the $Zn(OH)_2$colloids dissolves into Zn^{2+} and OH^- according to reaction stage 2. When the concentration of Zn^{2+} and OH^- reaches the super saturation degree of ZnO, ZnO nuclei will form according to reaction stage 3. The process was carried at variable temperature. Finally, dehydration of the precursor and followed by recrystallization, produced crystallites of ZnO.

Stage 1: $Zn(NO_3)_2 \cdot 6H_2O + 2NaOH \rightarrow Zn(OH)_2(gel) + 2NaNO_3 + 6H_2O$

Stage 2: $Zn(OH)_2(gel) + 2H_2O \rightarrow Zn^{2+} + 2OH^- + 2H_2O \rightarrow Zn(OH)_4{}^{2-} + 2H^+$

Stage 3: $Zn(OH)_4{}^{2-} \rightarrow ZnO + H_2O + 2OH^-$

2.16 Native Defect Studies in ZnO

Defects can be defined as anything that breaks the symmetry of the perfect crystal lattice including point-like imperfections such as vacancies, substitutions, interstitials anti-sites and extended imperfections such as defects, planar defects, and bulk defects [34]. Some of the point defects in ZnO include hydrogen (interstitial and substitution), oxygen and zinc vacancies, and oxygen and zinc substitutions. Another potential defect in semiconductors is the surface. It can be considered as the biggest extended defect since most of the characterization techniques access the semiconductor through its surface. In the case of PL [70], for example, even though the penetration depth depends on the wavelength of the excitation source, the density of excited carriers is highest near the surface. Often surface states are involved nonradiative relaxation processes particularly its effect increases as the surface-to volume ratio increases and therefore it plays a key role in nanostructures materials [70]. The intrinsic defects are associated with deep level emissions such as oxygen vacancies or zinc interstitials [38]. Notably, the oxygen vacancies and interstitials were induced by the thermal treatment process and sol–gel method. Vanheusden

et al. found that oxygen vacancies are responsible for the green luminescence in ZnO [23]. Oxygen vacancies occur in three different charge states: the neutral oxygen vacancy (Vo^0), the singly ionized oxygen vacancy (Vo^+) and the doubly ionized oxygen vacancy (Vo^{++}) of which only Vo^+can act as the so called luminescent center [24].

However, excess oxygen vacancies in the host would inevitably destroy the crystallinity, which leads to quenching of the luminescence. The Zn vacancies and surface defects are the main structural defects appeared in the ZnO semiconductors, during their fabrication. It is believed that they generate trapping centers in the band gap leading to luminescence in the visible wavelength region [70]. The broadening of the emission peak could be attributed to both size distribution and increase in the surface to volume ratio. Recently, Zeng et al. reported that the blue emission can be interpreted by the transition of extended Zn_i (zinc interstitials) states [21]. Here, as for the improvement in utilizing for the efficiency of exciting photons in the radiative recombination leads to the strong blue emission band. A detailed discussion of point defects in ZnO is presented in a book by Morkoc and Ozgur [32].

2.17 Characterization Techniques

Different characterization techniques have been used to investigate different properties of the material. Here, SEM, TEM, XRD, PL and UV-Vis spectrophotometer were the major techniques used to characterize nanomaterial as presented in the following subsections.

2.17.1 X-ray Diffraction (XRD)

X-rays are electromagnetic radiation of wavelength about 1Å (10^{-10} m), which is about the same size as an atom. They occur in that portion of the electromagnetic spectrum between gamma-rays and the ultraviolet. The discovery of X-rays in 1895 enabled scientists to probe crystalline structure at the atomic level [1]. X-ray diffraction is a versatile, non-destructive analytical method for identification and quantitative determination of various crystalline forms, known as phases of compound present in powder and solid samples. Diffraction occurs as waves interact with a regular structure whose repeat distance is about the same as the wavelength. For example, light can be diffracted by a grating having scribed lines spaced on the order of a few thousand angstroms, about the wavelength of light. It happens that X-rays have wavelengths on the order of a few angstroms, the same as typical inter-atomic distances in crystalline solids. That means

X-rays can be diffracted from minerals which, by definition, are crystalline and have regularly repeating atomic structures. When certain geometric requirements are met, X-rays scattered from a crystalline solid can constructively interfere and producing a diffracted beam [21].X-ray diffraction provides structural and physical information of crystalline materials. In particular, XRD analysis can provide the crystalline quality and crystallographic planes of the given material.

It is the most useful of all diffraction methods and when properly employed, can yield a great deal of structural information about the material under investigation. Powder diffraction method involves the diffraction of monochromatic X-rays by a powder specimen. Monochromatic usually means a strong K_α characteristic component of the filtered radiation from an X- ray tube operated above the K_α excitation potential of the target material. A high resolution powder Diffractometer was employed for characterization and grain size determination. The powder diffraction of a substance is characteristic of the substance and forms a sort of fingerprint of the substance to be identified.

The fingerprint characterization of crystalline materials and the determination of their structure are the two fields where XRD has been mostly used. A beam of X-rays of wavelength λ is directed to the crystal at an angle θ to the atomic planes then the scattered ray is determined by Bragg's law. In Bragg's law, the interaction between X-rays and the electrons of the atoms is visualized as a process of reflection of X-rays by the atomic planes. This is an equivalent description of the diffraction effects produced by a three dimensional grating. The atomic planes are considered to be semi-transparent, that is, they allow a part of the X-ray to pass through and reflect the other part, the incident angle θ (called the Bragg angle) being equal to the reflected angle. The two reflected rays will reinforce each other, only when this path difference is equal to an integral multiple of the wavelength. If d is the inter-planar spacing, the path difference is twice the distance $d\sin\theta$. The Bragg condition for reflection can therefore be written as [59]:

$$n\lambda = 2d_{hkl}\sin\theta \quad (2\text{-}3)$$

Where,

n ≡Integer (order of diffraction)

λ ≡ The wavelength of the XRD beam

θ ≡ The Bragg incident angle with the plane of lattice

d_{hkl} ≡ Inter planar spacing between diffracting planes.

When the size of the individual crystal like is less than 0.1 μm, the term particle size is used. To find the average particle size, Scherrer formula is used [4]. The width of the diffracted curve increases with reduction in grain size of the material.

The width β is usually measured in radians, at intensity equal to half the maximum intensity. One can take β as half the difference between the extreme angles, at which the intensity is zero [5-6].

$$\beta = \theta_1 - \theta_2 \quad (2\text{-}4)$$

Where, θ_1 and θ_2 are the diffraction angles, β is the full width at half maximum of the peak

The average grain size is calculated from the Scherrer formula:

$$D = \frac{0.9\lambda}{\beta cos\theta}, \quad (2\text{-}5)$$

Where,λ is the wavelength of CuK_α line (1.54056Å), θ is the diffraction angle, β is the full width at half maximum of the peak and D is the average particle size.

2.17.2 Scanning Electron Microscope (SEM)

The scanning electron microscope (SEM) is a type of electron microscope capable of producing high resolution images of a sample surface by scanning it with a high-energy beam of electrons. Due to the manner in which the image is created, SEM images have a characteristic three-dimensional quality and are useful for judging the surface structure of the sample. This method usually is applied to get information about the grain size, surface roughness, porosity, particle size distributions, material homogeneity, and inter metallic distribution and diffusion [47]. The electrons interact with the atoms to make the sample producing signals that contain information

about the sample's surface topography, composition and other properties such as electrical conductivity [1].

In a typical SEM configuration, electrons are thermionically emitted from a tungsten or lanthanum hexaboride LaB_6 cathode filament towards an anode; alternatively electrons can be emitted via field emission (FE). The electron beam, which typically has an energy ranging from a few KeV to 50KeV, is focused by two successive condenser lenses into a beam with a very fine spot size (~ 5nm) [61]. The beam then passes through the objective lens, where pairs of scanning coils deflect the beam either linearly or in a raster fashion over a rectangular area of the sample surface. As the primary electrons strike the surface they are inelastically scattered by atoms in the sample. Through these scattering events, the primary beam effectively spreads and fills a tear-drop shaped volume, known as the interaction volume, extending about 1µm to 5µm into the surface [61].

Interactions in this region lead to the subsequent emission of electrons which are then detected to produce an image. The most common imaging mode monitors low energy (<50eV) secondary electrons. Due to their low energy, these electrons must originate within a few tenths of a nanometer from the surface. Because the secondary electrons come from the near surface region, the brightness of the signal depends on the surface area that is exposed to the primary beam. This surface area is relatively small for a flat surface, but increases for steep surfaces. Thus steep surfaces and edges (cliffs) tend to be brighter than flat surfaces resulting in images with good three-dimensional contrast. Using this technique, resolutions of the order of 5nm are possible.

In addition to the secondary electrons, backscattered electrons (essentially elastically scattered primary electrons) can also be detected. Backscattered electrons may be used to detect both topological and compositional details, although due to their much higher energy (approximately the same as the primary beam) these electrons may be scattered from fairly deep within the sample. This results in less topological contrast than for the case of secondary electrons. However, the probability of backscattering is a weak function of atomic number, thus some contrast between areas with different chemical compositions can be observed especially when the average atomic number of the different regions is quite different.

2.17.3 Transmission Electron Microscope (TEM)

TEM is a microscopy technique whereby a beam of electrons is transmitted through an ultra-thin specimen, interacting with the specimen as it passes through it. The energy of electrons in TEM determines the lateral spatial resolution and the relative degree of penetration of electrons in specific samples. In addition to the capability of structural characterization, TEM has been explored for a wide range of applications in nanomaterial [24]. This includes the determination of the crystal structure and lattice parameter of individual nanomaterial and the measurement of mechanical properties of individual nanoparticles and nanowires [21].

In a typical TEM configuration, the electrons from the electron gun are accelerated to very high voltages (100 – 200 keV) which are allowed to pass through a specimen and focusing lenses. The wave length of electrons depends on the acceleration voltages. As an electron wave penetrates the sample, the resulting diffraction pattern reveals the structure of the observed sample [60].

The lens-systems consist of electronic coils generating an electromagnetic field. The ray is first focused by a condenser. It then passes through the specimen, where it is partially deflected. The degree of deflection depends on the electron density of the specimen. The greater the mass of the atoms, the greater is the degree of deflection. The TEM has the advantage that it is able to resolve to the order of a few angstroms [62].

2.17.4 Photoluminescence (PL)

PL is a process in which a substance absorbs photons and then re-radiates photons. PL is a non-destructive technique requiring no or little preparation of a sample. Different types of samples (powder, liquid or bulk semiconducting material) can be characterized. PL measurements are usually performed using two different excitation conditions. Firstly, when excitation is with a continuous beam, the material can reach a steady state. The PL measured under these conditions, called continuous wave (CW) or steady state PL, provides information mainly on the position of the electronic levels participating in the radiative recombination processes. Secondly, when PL is excited using light pulses of suitable duration, time-resolved PL (TRPL) is obtained and the excited state lifetime, which provides information on carrier dynamics and recombination kinetics, can be extracted. For CW-PL, the sample is excited by a laser with energy greater than its band gap and the luminescence intensity is measured as a function of wavelength or energy.

The heart of this optical measurement system is a monochromatic, which is used to differentiate between emissions at different photon energies, resulting in a plot of light intensity as a function of energy [63, 69].

Optical measurements provide information both about the host semiconductor, through intrinsic optical processes, and about the wide variety of impurities or defects which are endemic in all real semiconductor materials, through extrinsic optical processes. It is particularly suited for the detection of shallow-level impurities, can also be applied to certain deep-level impurities/defects, provided that their recombination is radiative [16].

2.17.5 Ultra Violet-Visible Absorption Spectroscopy (UV-Vis)

The electronic band structure of semiconductors and metals is determined by their optical properties. The optical absorption is a result of interaction between the material and light. When a frequency of light is in resonance with the energy difference between states the transition allowed or partly allowed by selection rules, a photon is absorbed by the material. This results in a decrease of transmission or an increase in absorbance of the light passing through the sample. By measuring the transmission or absorbance of sample as a function of the frequency of the light, one can obtain a spectrum characteristic of the material [63].UV-Vis absorption spectroscopy is the measurement of the attenuation of a beam of light after it passes through a sample or after reflection from a sample surface. Absorption measurements can be at a single wavelength or over an extended spectral range. Ultraviolet and visible light are energetic enough to promote outer electrons to higher energy levels, and UV-Vis spectroscopy is usually applied to molecules or inorganic complexes in solution. The UV-Vis spectra have broad features that are of limited use for sample identification but are very useful for quantitative measurements. The concentration of analyze in solution can be determined by measuring the absorbance at some wavelength. The Beer-Lambert law states that the absorbance of a solution is directly proportional to the solution's concentration. Thus, UV/VIS spectroscopy can be used to determine the concentration of a solution. The method is most often used in a quantitative way to determine concentrations of an absorbing species in solution, using the Beer-Lambert law [69]:

$$\log\left(\frac{I}{I_0}\right) = -\alpha \qquad \text{or} \qquad I = I_0 e^{-\alpha}, \tag{2-6}$$

Where$\alpha$is the measured absorbance, I_0 is the intensity of the incident light at a given wavelength and I is the transmitted intensity. The optical absorption coefficient was determined based on the band-gap energy (Eg). The band gap energy (Eg) of the synthesized ZnO nanoparticles was obtained using the relation [57]:

$$E_g(eV) = \frac{hc}{\lambda} = \frac{1240\ \text{eV.nm}}{\lambda} \tag{2-5}$$

Where, E_g is the band gap energy in electron volts and λ is wavelength (nm).The energy band gap (E_g) values are given in Table 4-1.The fundamental absorption method refers to band to band transitions by using Mott and Davis relation of Equation [47].For photon energies just above fundamental edge, the absorption coefficient follows the standard relation.

$$\alpha h\nu = A(h\nu - E_g)^n \tag{2-6}$$

Where A is a constant related to the extent of the band tailing, α– absorption coefficient, $h\nu$ – photon energy, E_g –energy band gap and n = 1/2 for allowed direct transition, n= 2 for allowed indirect transition and Eg is the energy gap between the valence band and the conduction band.

2.18 Application of Nanoparticles

Zinc oxide has attracted huge research effort due its potential versatile applications in ultraviolet (UV) photo detectors, chemical sensors, transparent electronics, spintronic, UV light emitters, surface acoustic devices, piezoelectric transducers, mechanical resonators, short-wavelength electronics, field effect transistors, logic gates, optical memory, light emission diodes, photovoltaic devices, superconductors, UV polymer Nano composites, bacteria DNA detection, neuro networks, hydrogen fuel engine system, water treatment and rubber nano-accelerators [22].

Chapter 3

Materials and Methodology

3.1 Experimental Site

The synthesis of zinc oxide nanoparticles was conducted at Adama Science and Technology University, ASTU chemistry post graduate and research laboratory. All the characterizations techniques of ZnO prepared samples by using X-ray diffraction (XRD), scanning electron microscope (SEM), transmission electron microscope (TEM), photoluminescence (PL)and ultra-violet (UV) Visible absorbance spectrophotometer were done at Sri Venkateswara University, Tirupati, India.

3.2 Apparatus Used

The apparatus used in this experiment were Glass Beakers, Magnetic stirrer with hot plate, Magnet pellets, Thermometer, Electronic balance, Universal drying oven, Spatula, Tong, Sample holder, Clean and White paper, Muffle furnace and Small mortar pestle.

3.3 Chemicals Used

The chemicals used in this work were purchased from Fine Chemical General Trading PLC and Neway PLC and used as-received (i.e. no further purification was attempted). The zinc nitrate hexahydrate ($Zn(NO_3)_2 \cdot 6H_2O$) was used as zinc precursors. Sodium hydroxide (NaOH) of was used as the hydroxide sources. Methanol(CH_40) (98%) was used as solvents. Methanol and sodium hydroxide take care for the homogeneity and PH value of the solution and helps to make a stoichiometric solution to get zinc oxide nanoparticles. Citric acid ($C_6H_8O_7.H_2O$) was used as passivating agents.

Table 3-1: Materials requirements for synthesis of ZnO Nano powder

Chemical name	Chemical formula	Mole required	Material taken
Zinc nitrate hexahydrate	$Zn(NO_3)_2.6H_2O$	0.01482	4.41g
Sodium hydroxide	NaOH	0.01475	0.59g
Methanol	CH_3OH	−−	50ml
Citric acid	$C_6H_8O_7.H_2O$	0.020	3g

3.4 Methods of Sample Preparation

The glass beakers were first cleaned and rinse with distilled water and dried in dry oven. All the materials and solvents were weighted with help of electronic weighing balance and mixed in cleaned beakers. The synthesis of ZnO in presence of surfactants can be summarized as:

The proposed ZnO powder synthesis was 5g and from the given material requirements found to:

$$\leftrightarrow m_{Zn(NO_3)_2.6H_2O}=\frac{m(Zn(NO_3)_2.6H_2O)}{\text{total molar mass}}\times 5g$$
$$=\frac{297.48}{337.48}\times 5g$$
$$=4.41g$$

$$\leftrightarrow m_{NaOH}=\frac{mNaOH}{\text{total molar mass}}\times 5g$$
$$=\frac{40}{337.48}\times 5g$$
$$=0.59g$$

Therefore, a 4.41g, zinc nitrate hexahydrate was dissolved in the 50ml of methanol at room temperature to at approximately~33℃. Then the solution was continuously stirred for 30minutes using magnetic stirrer to dissolve the zinc nitrate hexahydrate completely. After dissolution of zinc nitrate hexahydrate, 0.59g of NaOH pellets was added with constant stirring, drop by drop slowly touching the walls of the vessel at the same temperature. This reaction was allowed to continue for 20minutes until complete addition of NaOH. During the reaction citric acid was added to the solution at the same temperature with gentle stirring for 6hs by using magnetic stirrer with hot plate. After the reaction completed, reaction mixture allowed cooling to room temperature. The nanoparticles obtained were then dried in dry oven at approximately ~55℃ for 20-24hrs and then zinc hydroxide was completely converted into zinc oxide. Finally, heated sample was then grinded and calcinated under various annealing temperatures for 5hrs.

Illustration of the schematic flow chart of synthesizing ZnO nanoparticles:

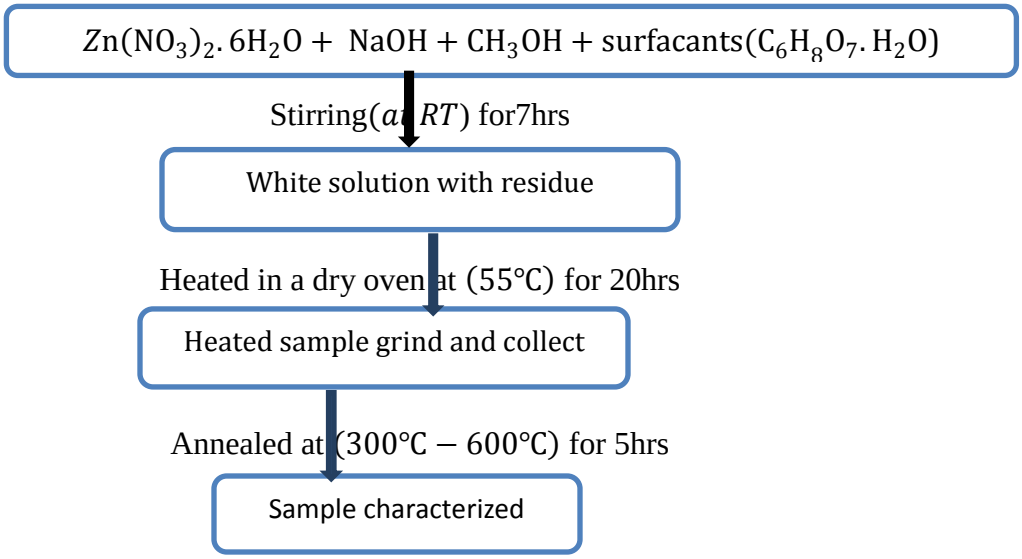

Figure 3-1: Flow chart of the synthesis of ZnO nanoparticles by sol-gel process

Citric acid: Citric acid was used to study the effects of surface passivation on the morphological, crystalline and optical properties. The citric acid was added to the solution during the preparation of samples. In this case, where citric acid is used more fine powders were obtained. Looking at XRD patterns of samples (Figure 3-1), it can be seen that citric acid enhances the crystallization process at lower temperatures but did not influence essentially the particles size.

Annealing: Annealing was performed for fixed time at temperatures ranging from 300°C to 600°C in air and the effects on the optical and structural properties were investigated. In all cases, the annealing was conducted in muffle furnace.

3.5 Characterization Methods of Nanoparticles

A large number of techniques can be employed for ZnO nanoparticles characterization. The most common techniques used in this work were x-ray diffraction (XRD), Scanning electron microscope (SEM), Transmission electron microscopy (TEM), Photoluminescence spectroscopy (PL) and Ultraviolet–visible spectrophotometer (UV-Vis). These techniques are;

1. Structural Characterization:
   - X-ray Diffraction(XRD)
   - Scanning electron microscopy(SEM)
   - Transmission electron microscopy(TEM)

2. Optical Characterization:
   - UV-Visible Absorbance Spectroscopy (UV-Vis)
   - Photoluminescence spectroscopy (PL)

3.5.1 X-ray Diffraction (XRD)

The X-ray diffraction (XRD) pattern of ZnO nanoparticles was obtained using a Seifert 3003TT system with X-ray Diffractometer (XRD) by generating CuK_α radiation (λ = 1.5406Å) at Sri Venkateswara, India. This technique was used to determine the crystalline phase of the synthesized material. Small amount of sample in powder form was used for the analysis. An X-ray generator was operating at a voltage of 40KV and applied a current of 35mA at room temperature (25^{o}C). Intensities were measured at room temperature in steps of 0.01, over the range of $5^0 \leq 2\theta \leq 80^0$. The Diffractometer is connected to a computer for data collection and analysis. Schematic of Seifert 3003TT X-ray. Diffractometer used was shown in Figure 3-2.

Figure 3-2: Schematic of Seifert 3003TT X-ray Diffractometer.

In addition, by applying Scherer's formula, the size of the crystallite of the ZnO samples were found to be same as the value measured by particle size analyzer.

$$D = \frac{0.9\lambda}{\beta \cos\theta,} \qquad (3\text{-}1)$$

Where, $D$is the average particle size, λ wavelength (1.54A°), βull maxima half width andθi diffraction angle. The peaks of the X-ray diffraction pattern can be compared with the standard available data for the confirmation of the structure.

3.5.2 Scanning Electron Microscope (SEM)

The scanning electron microscope (SEM) is a type of electron microscope capable of producing high resolution images of a sample surface. A SEM instrument used in this work is shown in Figure 3-3.

Figure 3-3: Schematic instrument of Scanning Electron Microscope.

In a typical SEM configuration, the electron beam, which typically has an energy ranging from a few KeV to 50KeV, is focused by two successive condenser lenses into a beam with a very fine spot size (~ 5nm). The beam then passes through the objective lens, where pairs of scanning coils deflect the beam either linearly or in a raster fashion over a rectangular area of the sample

surface. The spatial resolution of the SEM depends on the size of the electron spot which in turn depends on the magnetic electro-optical system which produces the scanning beam. The resolution is also limited by the size of the interaction volume, or the extent of material which interacts with the electron beam. The spot size and the interaction volume are both very large compared to the distances between atoms, so the resolution of the SEM is not high enough to image down to the atomic scale.

As the primary electrons strike the surface they are inelastically scattered by atoms in the sample. Through these scattering events, the primary beam effectively spreads and fills a tear-drop shaped volume, known as the interaction volume, extending about 1µm to 5µm into the surface. Interactions in this region lead to the subsequent emission of electrons which are then detected to produce an image.

In addition to the secondary electrons, backscattered electrons (essentially elastically scattered primary electrons) can also be detected. Backscattered electrons may be used to detect both topological and compositional details, although due to their much higher energy (approximately the same as the primary beam) these electrons may be scattered from fairly deep within the sample. This results in less topological contrast than for the case of secondary electrons. However, the probability of backscattering is a weak function of atomic number, thus some contrast between areas with different chemical compositions can be observed especially when the average atomic number of the different regions is quite different.

3.5.3 Transmission Electron Microscopy (TEM)

The TEM has the advantage that it is able to resolve to the order of a few angstroms. In this work a HF-2000 (set in Figure 3-4) is used to study the morphology of the nanoparticles. The samples were examined under the TEM after dispersing them in methanol and placing a few drops of the mixture in the Cu grid.

Figure 3-4: Schematic Transmission Electron Microscope

Principles of TEM; the electrons from the electron gun are accelerated to very high voltage (100 – 200keV) which are allowed to pass through a specimen and focusing lenses. The lens-systems consist of electronic coils generating an electromagnetic field. The ray is first focused by a condenser. It then passes through the specimen, where it is partially deflected. The degree of deflection depends on the electron density of the specimen.

The greater the mass of the atoms, the greater is the degree of deflection. If the intermediate lens is adjusted so that its object plane is the image plane of the projector lens, then an image is projected onto the viewing screen. If the back focal plane of the objective lens acts as the object plane for the intermediate lens, then the diffraction pattern is projected in the viewing screen [7].

3.5.4 Photoluminescence (PL) Spectroscopy

PL is a convenient technique requiring a suitable source of optical excitation, a monochromatic and a suitable detector for the emitted light. The photoluminescence spectra of the powder samples of the present system were recorded in the wavelength range 325-600 using an F-3010 Hitachi fluorescence spectrophotometer. The light emitted from the Xe-lamp enters the excitation monochromatic.

The beam splitter splits the light emerging from the excitation monochromatic and a fraction of it is directed to the monitor detector. A shutter is provided between the excitation monochromatic and the sample, which is placed in the optical path as commanded from the operation panel. All the driving components, i.e., the wavelength drive motors, slit control motors and rotary solenoids for shutter are operated by signals sent from the computer.

3.4.5 Ultra Violet-Visible Spectroscopy (UV-Vis)

An Ultraviolet-Visible (UV-Vis) spectrophotometer was used to measure the absorption edge of the synthesized ZnO nanoparticles. For this purpose, the small amount of ZnO Nano powder mixed with methanol was shaking using quartz cuvette. Then after, mount it into UV-Vis spectrophotometer. The absorbance was measured over the wave length range of 200nm-500nm.

Chapter 4

Results and Discussion

The synthesized ZnO nanoparticles were characterized using X-ray diffraction (XRD), Scanning electron microscope (SEM), Transmission electron microscope (TEM), UV-Vis absorbance spectrophotometer and Spectrophotometer.

4.1. X-ray Diffraction (XRD)

X-ray diffraction is a non-destructive technique that reveals the crystal structure of the material under analysis. Figure 4-1reveal that the XRD patterns of ZnO nanoparticles has Wurtzite hexagonal structure. All XRD diffraction peaks of ZnO powders shown was in a good agreement with hexagonal structure of zincite phase reported in JCPDS File Card No.05-0664.Furthermore, we could not find any diffraction peak corresponding to any impurity phase within the limit of instrumental sensitivity, indicating that the high purity ZnO was obtained. The peak positions do not show any measurable change, while the intensities of the peaks increase with increasing temperatures.

The diffraction peaks at the diffraction angles of 31.79^0, 34.40^0, 36.23^0, 47.52^0, 56.58^0, 62.85^0, and 67.96° matches to the reflection from (100), (002), (101), (102), (110), (103) and (200) crystal planes respectively which shows the hexagonal wurtzite structure of ZnO nanoparticles (Lv *et al.*, 2011).The diffraction peaks of ZnO nanoparticles at 300°C are broadened and the average crystallite size was estimated to be 15.31nm. The XRD peaks appear to be sharper with decreased full width at half the maximum (FWHM), indicating possible increase in crystallite size. The sharp diffraction peaks clearly indicate good crystallinity of the ZnO nanoparticles. However, the full-width at half maximum (FWHM) had a tendency to decrease with increasing the annealing temperature as result diffraction peaks become stronger and sharper, thereby indicating that the crystal quality has been improved and the size of particles become bigger (see Figure 4-1).The value of the interatomic spacing d_{hkl} between similar planes, for an XRD peak can be determined from the 2θ angle by applying Bragg‟s Law:

$$2d_{hkl}\sin\theta = n\lambda, \qquad (4\text{-}1)$$

Where d_{hkl} is the inter planar spacing between planes called *lattice parameter*, λ is the wave length of x-ray for Cu target Kα radiation; θ is Bragg‟s diffraction angle and n is integer ($n = 1$, for first order diffraction).

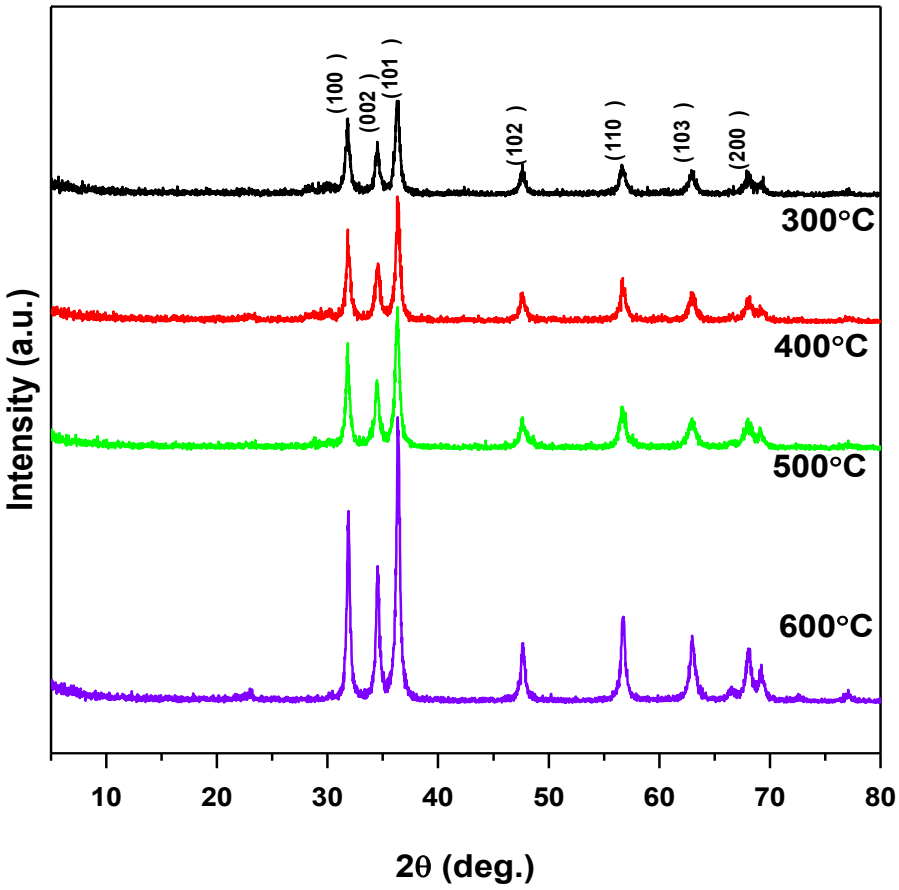

Figure 4-1: XRD pattern of ZnO nanoparticles after calcinations at (300℃ to 600℃)/5hr

In conclusion; with increasing the annealing temperature, the intensity of the major diffraction peaks increased indicating that the crystallization of ZnO nanoparticles was improved at higher temperatures. In addition, our results and previous reports [22, 23] also show that increasing the heat treatment temperature improves the crystallization of ZnO nanoparticles. The diffraction lines of ZnO were broadened, and diffraction broadening was found dependent on Miller indices of the corresponding sets of crystal planes. For most samples the diffraction line (002) is narrower than the line (101), and (101) is narrower than the line (100).

This indicated an asymmetry in the crystallite shape. A definite line broadening of the diffraction peaks is an indication that the synthesized materials are in nanoscale range. The crystallite size of the ZnO samples was found to be in the range15.31–30.63nm using the Scherrer equation (Table 4-1).This result is associated with the grains growing more easily when the temperature is higher. The lattice parameter for hexagonal ZnO nanocrystals;

$$d_{hkl} = \frac{1}{\sqrt{\frac{4}{3}\frac{(h^2+hk+k^2)}{a^2} + \frac{l^2}{c^2}}}, \qquad (4\text{-}2)$$

Whereh, k and $l$are the Miller indices; and $d_{hkl}$is the lattice parameter corresponding to the given miller indices. This inter-planar distance were estimated from the (101) and (102) plane using the equation Eqn. (4-2)is$a = 0.3258nm,\ c = 0.5199nm$.

4.2 Scanning Electron Microscopy (SEM)

In the Figure 4-2 (a) and (b) below, the SEM micrographs clearly depicts the spherical shape of the ZnO nanoparticles. These figure show the powder scanning electron microscopy (SEM) images of the resultant products obtained at (a) 300℃/$5hr$ and (b) 500℃/$5hr$. By increasing temperature, morphologies of the synthesized ZnO products can be changed, at300℃, a nanoparticle with $1\mu m$dimension was obtained, but at 600°C with 500nms dimensions was obtained. Thereby, the effects of the temperature in the starting solution on the morphology and shape of as-synthesized ZnO nanoparticles were shown in Figure 4-2. When the annealing temperature increases from 300℃ to 600℃, obviously, the crystallinity of the products will be improved.

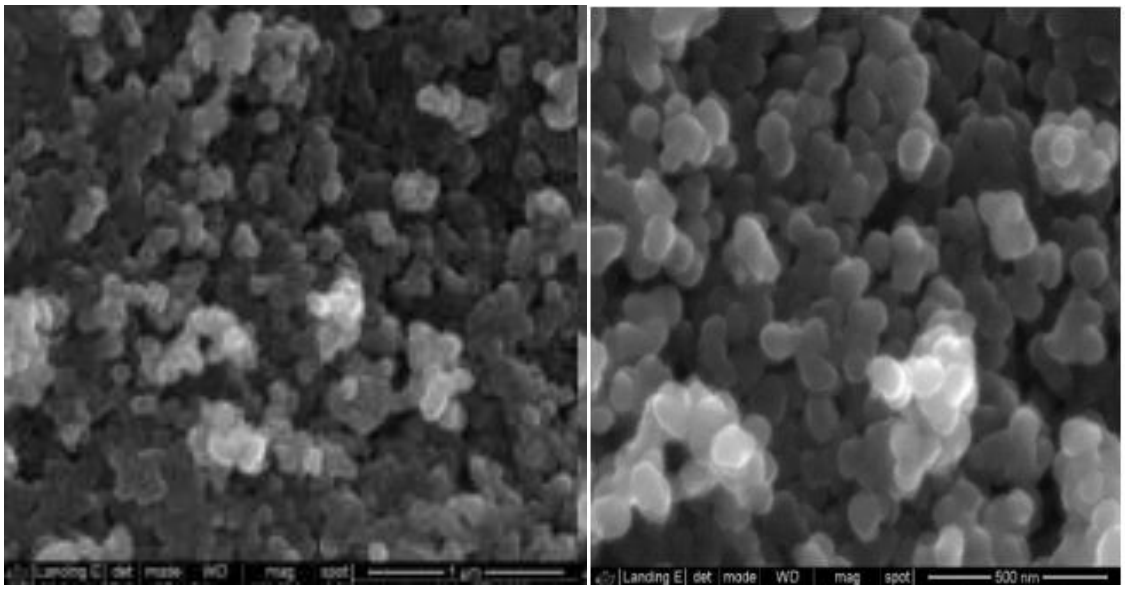

(a) (b)

Figure 4-2: The SEM images of the synthesized ZnO nanoparticles at (a) 300℃/*5hr* and (b) 500℃/*5hr*.

4.3 Transmission Electron Microscopy (TEM)

TEM analysis has been the most popular method for the estimation of average particle size in nanomaterial and it also provided information on element and compound structure, images were high-quality and detailed and able to yield information of surface features such as size and structure. Therefore, it has been extensively used in the present work. As the Figure 4-3 clearly showed that transmission electron microscope produced a high resolution, black and white images.

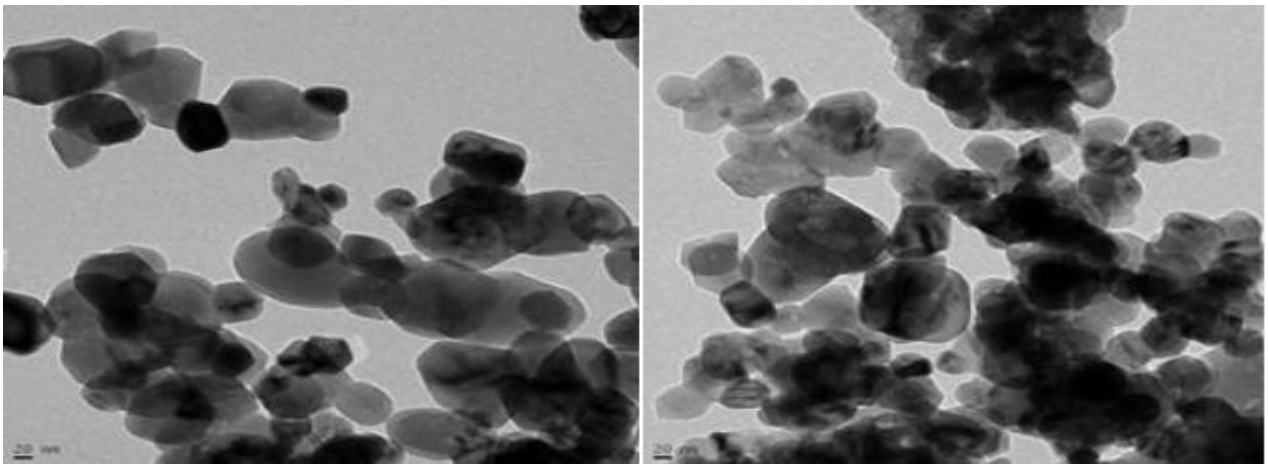

(a) (b)

Figure 4-3: TEM image of ZnO nanoparticles at 500^0C/5hrs and 600^0C/5hrs.

Therefore, the TEM images and the histogram result indicated that the particle size distribution range from smaller to larger particles that means it is a polydisperse material. As Figure 4-3 shows, The TEM image clearly showed very small amount of agglomeration or clustering. The images clearly showed hexagonal nanoparticles, which in accord with the XRD result. The average particle size of the synthesized ZnO nanoparticles was found to be 20nmwhich confirms with the average crystallite size of the prepared ZnO samples was found to be $20 \pm 2.63\ nm$ using the Scherrer equation.

4.4 Ultra Violet-Visible (UV-Vis) Absorbance Spectroscopy

As indicated in Figure 4-4, the UV-Vis spectra from synthesized ZnO nanoparticles show absorbance at different regions (UV-region) which is in agreement with the results obtained by (Giri *et al.,* 2011). The absorption of a photon, leading to excitation of an electron from the valence band to the conduction band (band to band transition), is associated with the band gap energy UV emission at 366.96nm. UV emission band at 375.96nm (inset in Figure 4-4) showed that the near band emission was caused by the transition from conduction band to valence band (free excitons). Moreover, the full width at the half maximum (FWHM) decreased slightly with increasing the temperature as shown in Figure 4-4. This should be one reason why the increased intensity peaks of UV emission is associated with the grain size and crystal orientation [37].

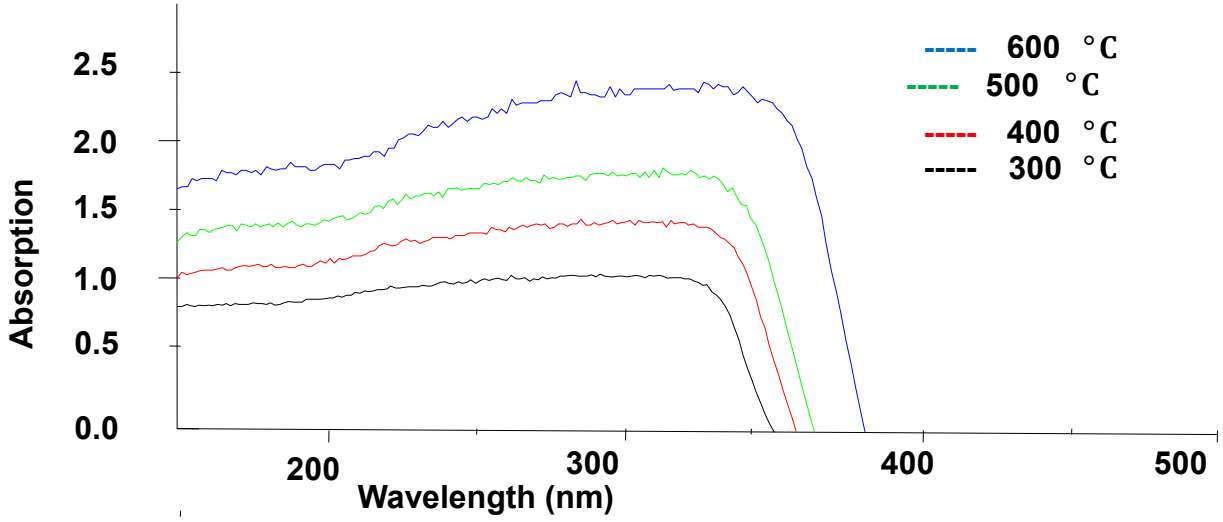

Figure *4-4*: Optical absorption spectra of as prepared ZnO Nanoscale annealed at various temperatures

The calculated value for the band gap energy of the synthesized ZnO nanoparticles using Eqn. (2-5) was found to be 3.370eV, 3.344eV, 3.321eV & 3.298eV for the samples calcinated from 300℃- 600℃ respectively.Therefore, absorption edges for ZnO nanoparticles synthesized corresponding to increase in the crystal size.

Table 4-1: Energy band gap versus annealing temperatures.

Annealing temperatures	Wave length (nm)	Grain size (nm)	FWHM	Energy band gap (eV)
300℃	367	15.31	0.905	3.38
400℃	370.75	20.42	0.679	3.344
500℃	373	25.52	0.543	3.32
600℃	375.96	30.63	0.452	3.29

In conclusion, the optical absorption spectra of ZnO samples shown in Figure 4-4indicate that the increase in annealing temperatures shifted towards a longer wavelength in the absorption edge. Thereby, it indicates that band gap decreases with small value with increasing annealing temperature.

4.5 Photoluminescence (PL) Spectroscopy

Photoluminescence is a sensitive nondestructive technique to investigate the intrinsic and extrinsic defects in a semiconductor. Figure 4-5showsthe PL spectra of the as-synthesized ZnO nanoparticles with an excitation wavelength of 325nm from Xe lamp source.

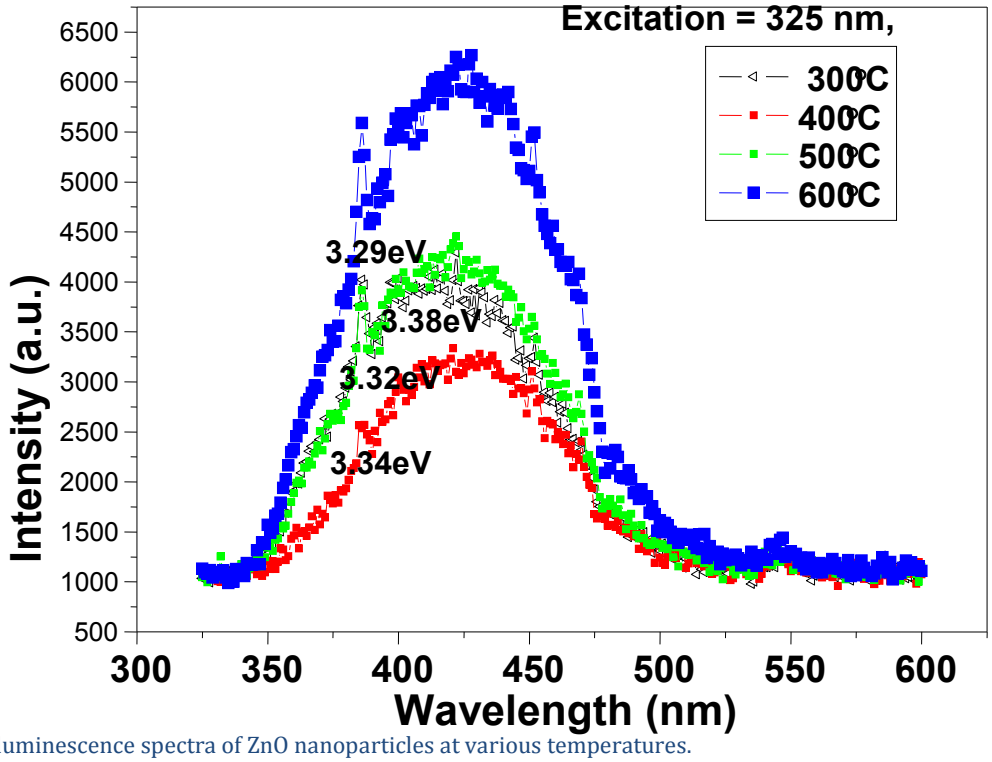

Figure 4-5: Photoluminescence spectra of ZnO nanoparticles at various temperatures.

In this spectrum, the as-grown sample turns to be broad and dominant in the UV region. However, the as-synthesized ZnO nanoparticles contain emission bands centered at 375.96nmcorresponding to the near-band edge (NBE) emission. The NBE emission is attributed to the radiative recombination of a hole in the valence band and an electron in the conduction band [19]. The strong PL peak emission at 366.96nm is well corroborated with the previous report on ZnO quantum dots [20], which was attributed to the free excitons recombination in ZnO. In addition, a much weaker peak is located at 550nm which is attributed to the surface defect from oxygen vacancies or Zn_i [22]. During thermal treatment at high temperatures (600°C), although the adsorbed functional groups are removed, the concentration of intrinsic defects is expected to increase. Under this the same excitation conditions, the defect emission will resulting in an absolute and a relative increase in the DLE. Therefore, the results of PL spectrum show that the varying of emission intensities confirms that the annealing temperatures are successfully produce high optical quality of ZnO nanoparticles.

In conclusion; in the present study, the PL intensity emission peak increased when the calcinated temperature was raised from 300℃, to 600℃ for 5h in air. The ZnO nanoparticles at 600℃ show the best crystallize quality suggesting that increasing the annealing temperature not only raised the crystalline quality but also improved the optical properties.

Chapter 5

Conclusions and Future Plan

In this thesis, the method of sample preparation and growth processing procedure were mainly carried out in chapter 3 to produce ZnO nanopowders. The prepared ZnO powders were then characterized using x-ray diffraction (XRD), scanning electron microscope (SEM), transmission electron microscope (TEM), photoluminensce (PL) and UV-Vis absorption measurement in chapter 4. However, in this chapter the salient results were summarized followed by future outlook and suggestions.

The x-ray diffraction (XRD) results showed that the obtained ZnO nanoparticles were composed of hexagonal wurtzite phase with very good crystallinity, and the average particle size was found to 20nm $\pm$2.63nm for ZnO nanoparticles. The standard deviation 2.63nm refers to errors may due to experiments or calculations. The scanning electron microscope (SEM) images depicts the powder to have spherical morphology and also showed the morphological homogeneity of the synthesized nanomaterial with very small amount branch structure. The transmission electron microscopy (TEM) clearly showed that the produced micrographs of ZnO nanoparticles are crystalline and some agglomerations. The average particle sizes investigated from TEM were found to be 20nm.

The grown ZnO nanoparticles UV optical spectra contain emission bands centered at 366.96nm, 370.75nm, 373.34nm and 375.94nm corresponding to the near-band edge (NBE) emission energy were 3.38eV, 3.34eV, 3.32eV and 3.29eV respectively, showed that the fundamental absorption edge shifted towards lower wavelengths (blue region) with increasing annealing temperatures indicating that the presence of a small blue shift in the present samples providing sample evidence to the formation of nanoparticles and to the signature of size quantization effect, which shows that the size of the particles is in the nano-region. The photoluminensce (PL) spectra revealed the broad and dominant in the UV region. It is suggested that annealing at temperatures of 500^0C and 600^0C leads to an improvement in the crystalline and optical quality (due to the higher PL intensity compared to the as grown sample). From Figure 4-5 we can see that the high peak position systematically shifts to higher energy band as the annealing temperature was increased from 300°C to 600°C.

Therefore, ZnO nanoparticle grown by sol-gel method has high quality and efficiency for blue/ ultra-violet based operating optoelectronic devices application, (e.g. LED, laser diodes, and photodiodes). For the purpose, we concluded that temperature is an important thermodynamic factor that plays a key role in controlling the growth rate of a crystal quality and limits optical properties, (e.g. at higher temperatures, the Zn and O atoms arriving at the stable nuclei have sufficient energy to move around on the surface and find low energy sites whereas if the temperature is too low, growth may not occur or atoms cannot find low energy surface sites).

Furthermore, in the future the effect of doping that will improve optical quality higher than temperature effect and the mechanism of operating ZnO based optoelectronic devices will be studied.

6 References

[1]Yang, L.2008.Synthesis and optical properties of ZnO nanostructures. Thesis at Linköping University, Liu-Tryck Linkoping. Pp. 1-20.

[2] Hernandezbattez, A., R. Gonzalez, J. Viesca, J. Fernandez, J. Diaz Fernandez, A. MacHado, R. Chou and J. Riba, 2008. CuO, ZrO2 and ZnO nanoparticles as anti-wear additive in oil lubricants. Wear. 265 (3–4): 422.

[3] Bougrine, A., A. El Hichou, M. Addou, J. Ebothe, A. Kachouane and M.Troyon, ., "Structural, optical and cathodolumunisence characteristics of un doped and tin doped zinc oxide prepared by spray pyrolysis," *Mater. Chem. Phys.,* vol. 80, pp. 438-445, 2003.

[4] Cordaro, J.F., Y. Shim and J.E. May, 1986. Structural and optical properties of ZnO Nano rods prepared by chemical bath deposition method. *J. Appl. Phys*. 60: 4186-90.

[5] Huang, M.., S. Mao, H. Feick, H. Yan, Y. Wu, H. Kind, E. Weber, R. Russo and P. Yang, 2001. Electrodeposited ZnO films with high UV emission properties Science, 292: 1897-9.

[6] Pan, Z.W., Z.R. Dai and Z.L Wang, 2001. Nano belts of semiconducting oxides Journal of Science. 291:1947-49.

[7] Johnson, J.C., H. Yan, R.D. Schaller, P.B. Petersen, P. Yang and R.J Saykally, 2002. Nano Lett. 2: 279-83.

[8] Govender, K., D.S. Boyle, P. O‟Brien, D. Binks, D. West and D. Coleman, 2002. Room temperature lasing observed from ZnO Nano columns grown by aqueous solution deposition. Adv. Mater., 14: 1221-24.

[9] Lao, J.Y., J.G. Wen and Z.F Ren, 2007. Zinc Oxide Nanostructures: Synthesis and Properties. Nano Lett. 2: 1287-91.

[10] He, S.T., J.N. Yao, P. Jiang, D.X. Shi, H.X. Zhang, S.S. Xie, S.J. Pang and H.J Gao, 2001.Langmuir, 17:1571-5.

[11] Sakohara, S., L.D. Tickanen and M.A. J. Anderson, 1992. J.Chem. Eng. 25: 598-603.

[12] Wang, C.C., Z. Zhang and J.Y. Ying, 1997. *Nanostructured Mater*. 9: 583. Wang, J., 2000. Analytical electrochemistry. Second edition Wiley-VC New York. 212:10158-0012.

[13] Bahnemann, D.W., C. Kormann and M.R.Hoffmann, "Kinetics of electrophoretic deposition for nanocrystalline zinc oxide coatings," *J. Phys. Chem.,* vol. 91, pp. 3789-98, 1987.

[14] Chittofrati, A. and E. Matijevic, 1990. Investigation of ZnO Nanowire Interfaces for Multi Scale Composites. J.Colloids Surf, 48: 65-78.

[15] Kumar, R.V., Y. Diamant and A. Gedanken, 2000. Mesoscale organization of CuO Nano slices: Formation of sphere. Chem.Mater. 12: 2301-5.

[16] Li, W.J., E.W. Shi, Y.Q. Zheng and Z.W.J Yin, 2001. Synthesis of ZnO nanoparticles by hydrothermal method. Mater. Sci. Lett., 20: 1381-3.

[17] Zhang, J., L.D. Sun, J.L. Yin, H.L. Su, C.S. Liao, and C.H.Yan, 2002. *Chem. Mater*.14: 4172.

[18] Pacholski, C., A. Kornowski and H. Weller, 2002. *Angew, Chem. Int. Edn*. 41: 1188-91.

[19] Azam, A., F. Ahmed, N. Arshi, M. Chaman and A.H. Naqvi, "Low temperature synthesis of ZnO nanoparticles using mechanochemical route.," *International Journal of Theoretical & Applied Sciences,* vol. 1(2, pp. 12-14., 2009.

[20] Crandell, B. C., 1996. Nanotechnology molecular speculation on global abundance. Cambridge, MA: MIT Press. 22: 269-273.

[21] Behera J.K., 2005. Synthesis and characterization of ZnO nano-particles. Master thesis submitted to department of physics, national institute of technology Rourkela, Orissa. Pp.1-19.

[22] Mahmud, S.B., 2008. Synthesis and characterization of zinc oxide nanostructures. Thesis submitted to University Sains Malaysia. Pp. 3-24.

[23] Kung, H.H. and E.I. Ko, 1996. Sol-gel synthesis and characterization of novel metal oxide nanomaterial for photo catalytic applications J. Chem. Eng. 64:203.

[24] Cao, G., 2004. Nanostructures and nanomaterial synthesis, properties and applications. Imperial College Press**,** London. pp 135–138.

[25] Chen, R., (2011). Synthesis of Zinc Oxide Nanostructures by Wet Oxidation Process. A thesis submitted to department of Chemical and Materials Engineering, University of Auckland: pp.22-23.

[26] Corriu, R. and R.T. Anh, 2009. Molecular chemistry of sol-gel derived nanomaterial. John Wiley and Sons Ltd, New York. 30(4): 809-812.

[27] Giri, P. K., S. Bhattacharyya, B. Chetia, S. Kumari, D. K. Singh and P. K. Iyer, 2011. High yield chemical synthesis of hexagonal ZnO nanoparticles and Nano rods with excellent optical properties. J. Nano science. Nanotechnology. 11: 1–6.

[28] Klein, L., 1994. Sol-Gel Optics processing and applications. Springer Verlag, Berlin.Vol.38, pp.45-6.

[29] Lv J., W. Gong, K. Huang, J. Zhu, F. Meng, X. Song and Z. Sun, 2011. Effect of annealing temperature on photo-catalytic activity of ZnO thin films prepared by sol-gel method. Super lattice and Microstructures, 50 (2): 98-106.

[30] C. Jagadish, S.J. Pearton, Zinc Oxide Bulk, Thin Films and Nanostructures: Processing, Properties and Applications. Austeralia: Elsevier Limited, 2006.

[31] D. M. Bagnall, Y. F. Chen, Z. Zhu, T. Yao, S. Koyama, M. Y. Shen, T. Goto., "Optically pumped
lasing of ZnO at room temperature," *Appl. Phys. Lett.*, vol. 70, p. 2230, 1997.

[32] H. Morkoc, U. Ozgur, *Zinc Oxide: Fundamentals, Materials and Device Technology.* ISBN: 978-3-527-40813-9, Ed. Germany: WILEY-VCH, Copyright @2009.

[33] N. H. Nickel, Evgenii Terukov, "ZnO: A material for micro-Optoelectronic applications," NATO science series, research output Vol. 194, 2004.

[34] U. Uzgur, Ya. I. Alivov, C. Liu, A. Teke, M. A. Reshchikov, S. Dogan, V. Avrutin, S.J. Cho, H. Morkoc, "A comprehensive review of ZnO materials and devices," *J. Appl. Phys.*, vol. 98, p.041301, 2005.

[35] M. H. Huang, Y. Wu, H. Feick, N. Tran, E. Weber, P. Yang, "Catalytic Growth of Zinc Oxide Nanowires by Vapor Transport," *Adv. Mater*, vol. 13, p. 113, 2001.

[36] JWu, S. C. Liu, "Low-Temperature Growth of Well-Aligned ZnO Nano rods by Chemical Vapor Deposition," *Adv. Mater.*, vol. 14, p. 215, 2002.

[37] S. Baruah, J. Dutta, "pH-dependent growth of zinc oxide Nano rods," *J. Crystal Growth*, vol. 31, pp. 2549-2554, 2009.

[38] C. Woll, "The chemistry and physics of zinc oxide surfaces," *Progress in Surface Science 82*, vol.82, pp. 55–120, 2007

[39] Y.Gu, I. L. Kuskovsky, M. Yin, S. O'Brien, G. F. Neumark, "Quantum confinement in ZnO Nano rods, Appl.Phys.Lett" vol. 85, p. 3833, 2004.

[40] J. G. Lu, Z. Z. Ye, J. Y. Huang, L. P. Zhu, B. H. Zhao, Z. L. Wang, Sze. Fujita, "ZnO quantum dots synthesized by a vapor phase transport process, Appl.Phys.Lett" vol. 88, p. 063110, 2006.

[41] K. Jacobs, D. Bali sky, P. Armand, P. Papet, "Low-temperature chemical bath deposition of crystalline ZnO," *Solid State Sci.*, vol. 12, pp. 333–338, 2010

[42] Z.M. Liao, H.Z. Zhang, Y.B. Zhou, J. Xua, J.M. Zhang, D.P. Yu, "Surface effects on photoluminescence of single ZnO nanowires," *Physics Letters A*, vol. 372, pp. 4505–4509,2008.

[43] L.L Yang, "Synthesis and Characterization of ZnO Nanostructures," Linkoping University, Linkoping, PhD thesis Dissertation No.1327, 2010.

[44] W. Z. Liu, H. Y. Xu, J. G. Ma, C. Y. Liu, Y. X. Liu , "Effect of oxygen-related surface adsorption on the efficiency and stability of ZnO Nano rod array ultraviolet light-emitting diodes ," *Appl.Phys. Lett.* vol. 100, p. 203101, 2012.

[45] T. Becker, S. Hovel, M. Kunat, C. Boas, U. Burghaus, C. Woll, "Interaction of hydrogen with metal oxides: the case of the polar ZnO (0001) surface," *Surface Science*, vol. 486, pp. L502–L506, 2001.

[46] B. Meyer, "First-principles study of the polar O-terminated ZnO surface in thermodynamic equilibrium with oxygen and hydrogen," *Phys. Rev. B*, vol. 69, p. 045416, 2004.

[47] L. Guo, S. Yang, C. Yang, P. Yu, J. Wang, W. Ge, G.K. L. Wong , "Highly monodisperse polymer capped ZnO nanoparticles: Preparation and optical properties," *App. Phys. Lett.*, vol. 76, p. 2901, 2000.

[48] J. Lee, A.J. Easteal, U. Pal, D. Bhattacharyy, "Evolution of ZnO nanostructures in sol–gel synthesis," *Current Applied Physics*, vol. 9, pp. 792–796, 2009.

[49] Z.N. Urgessa, O.S. Ouwafemi, J.R. Botha, "Effect of precursor concentration on the growth of ZnO nano arrays," *Physical B*, vol. 407, pp. 1543–1545, 2012.

[50] Z. Yang, Q.H. Liu, L. Yang, "The effects of addition of citric acid on the morphologies of ZnO nanorods," *Materials Research Bulletin*, vol. 42, pp. 221–227, 2007.

[51] Ji-W. Jang, S-Ho Jung, Bo R. Lee, E. Oh, K-H. Lee S. Cho, "Precursor Effects of Citric Acid and Citrates on ZnO Crystal Formation," *Langmuir*, vol. 25, pp. 3825-3831, 2009.

[52] V. S. Yalishev, Y. S. Kim, X. L. Deng, B. H. Park, Sh. U. Yuldashev, "Study of the photoluminescence emission line at 3.33eV in ZnO films," *J. Appl. Phys.*, vol. 112, p. 013528, 2012.

[53] J. Gao, X. Zhang, Y. Sun, Q. Zhao, D. Yu, "Compensation mechanism in N-doped ZnO nanowires ," *Nanotechnology*, vol. 21, p. 245703, 2010.

[54] J.S. Huang, C.F. Lin, "Influences of ZnO sol-gel thin film characteristics on ZnO nanowire arrays prepared at low temperature using all solution-based processing ," *J. Appl. Phys.*, vol. 103, p. 014304, 2008.

[55] W. Shan, W. Walukiewicz, J. W. Ager III, and K. M. Yu, H. B. Yuan, H. P. Xin, G. Cantwell, J. J. Song, "Nature of room-temperature photoluminescence in ZnO," *Appl. Phys. Lett.*, vol. 86, p. 191911, 2005.

[56] Bowman, M.J. and A.D. Booth, 1997. A review of methods for the examination of magnetic domain structure. *J. Materials Characterization.* 39: 139-167. Brinker, C.J. and G. W. Scherer, 1990. Sol-Gel Science: the Physics and chemistry of sol-gel processing. Academic Press, pp 1-10.

[57] El-Kemary, M., H. El-Shamy and I. El-Mehasseb, 2010. Photo catalytic degradation of ciprofloxacin drug in water using ZnO nanoparticles. *Alloys Compd*.433:237-240.

[58] Choy, J.H., E.S. Jang, J.H. Won, J.H. Chung, D.J. Jang and Y.W Kim, 2004. Hydrothermal route to ZnO Nano coral reefs and Nano fibers. *J. Appl. Phys. Lett*. 84, 287-289.

[59] Fulati, A., 2010. Mechanical characterization and electrochemical sensor applications of zinc oxide nanostructures. Thesis Printed by LiU-Tryck, Linköping. Pp. 4-23.

[60] Tonjic, A., 1999. High Resolution electron microscopy: image processing analysis of defects and grain boundaries in nanocrystalline materials*. Journal of Physics*. 46(3): Pp.435-461.

[61] Chang Shi Lao et al., Nano letters, 6(2006)263-266.

[62] http://en.wikipedia.org/wiki/Scanning_electron_microscope.

[62] http://en.wikipedia.org/wiki/Transmission_electron_microscopy.

[63] http://www.scribd.com/doc/21053651/Electronic-spectroscopy-UV-Visible.

[64] http://www.nanotechnologies.qc.ca/projects/ZnO/ZnO_nanostructures#more.

[65] http://anyfreepapers.com/free-research-papers/nanotechnology-research-aper.html.

[66] http://en.wikipedia.org/wiki/Nanotechnology.

[67] Cordaro, J.F., Y. Shim and J.E. May, 1986. Structural and optical properties of ZnO nanorods prepared by chemical bath deposition method. *J. Appl. Phys*. 60: 4186-90.

[68] Mott, N.F.; Gurney, R.W. *Electronic Processes in Ionic Crystals*; Oxford University press: Oxford, England, 1940; p. 141.

[69] S. Monticone, R. Tufeu, and A.V. Kanaev, "Complex nature of the UV and visible fluorescence of colloidal ZnO nanoparticles", *Journal of Physic Chemistry B*, Vol. 102, pp. 2854, 1998.

[70] D.C. Look, C.Co skun, B.Claflin, G.C. Farlow, "Electrical and optical properties of defects and impurities in ZnO," *Physical B*, vol. 340–342, pp. 32–38, 2003.